

Self-consistent dynamical maps for open quantum systems

Orazio Scarlatella^{1,2,3*}, Marco Schirò¹

1 JEIP, UAR 3573 CNRS, Collège de France, PSL Research University, 11 Place Marcelin Berthelot, 75321 Paris Cedex 05, France

2 Pritzker School of Molecular Engineering, University of Chicago, 5640 South Ellis Avenue, Chicago, Illinois 60637, U.S.A.

3 T.C.M. Group, Cavendish Laboratory, J.J. Thomson Avenue, Cambridge CB3 0HE, UK

* os444@cam.ac.uk

March 2, 2023

Abstract

In several cases, open quantum systems can be successfully described using master equations relying on Born and Markov approximations, but going beyond these approaches has become often necessary. In this work, we introduce the NCA and NCA-Markov dynamical maps for open quantum systems, which go beyond these master equations replacing the Born approximation with a self-consistent approximation, known as non-crossing approximation (NCA). These maps are formally similar to master equations, but allow to capture stronger couplings with the environment at very little extra numerical cost. To demonstrate their capabilities, we apply them to the spin-boson model at zero temperature for both a Ohmic and a sub-Ohmic environment, showing that they can both qualitatively capture its strong-coupling behaviour and be quantitatively correct at weak coupling, beyond what Born and Born-Markov master equations can do.

1 Introduction

The theory of open quantum systems, born to describe nuclear magnetic resonance (NMR) [1–3] and lasers [4, 5], is now of fundamental importance for the development of quantum devices [6–11], to describe chemical reactions [12–15], understand biological complexes [16–21] and to explore novel non-equilibrium quantum states [22–25].

For typical quantum optical systems [26], where the coupling with the environment is weak and the environment is unstructured, one can rely on Born-Markov master equations [2, 27–35] and on equivalent stochastic approaches [36–38]. Nevertheless, nowadays going beyond these approaches is necessary for a growing number of cases, including electronic transport problems [39–43], optomechanical resonators [44], quantum dots [45, 46], superconducting circuits [47–49] and quantum simulation platforms [50–54] where the system-bath coupling is strong and therefore non-Markovian dynamics [53, 55–59] and strong-coupling phenomena are expected.

Theoretical approaches beyond Born-Markov master equations have recently been developed, including phenomenological master equations [39–41, 60–62], but also microscopic approaches such as diagrammatic techniques [63–69] including diagrammatic Monte-Carlo [70–75], hierarchies of exact equations of motion [76–83] and matrix product states approaches [84, 85]. The latter microscopic techniques can be very powerful, but they are often computationally demanding

and are formally more involved than Born-Markov master equations, limiting their applicability in many practical cases.

On the other hand, in different contexts such as in textbook applications of many-body theory [86], often very simple non-perturbative approaches have been devised in the form of self-consistent approximations corresponding to partial resummations of perturbation theories, that can capture strong-coupling phenomena but still rely on simple equations. An example are the non-crossing approximations (NCA), that have been used for example for disordered systems [87], for quantum impurity models, both in and out of equilibrium [88–92], and for quantum transport problems [93–96]. In [97] a NCA has been formulated to conveniently capture the dynamics of quantum systems coupled simultaneously to a Markovian and to a non-Markovian environment.

In this work, we show how for generic open quantum systems the NCA of [97] can be used to upgrade the Born approximation, underlying standard master equations such as the Redfield [2] or Lindblad-Davies [27], and that it can also be combined with the usual Markovian approximation. The result is an equation for the dynamical map propagating the system density matrix, the NCA or NCA-Markov map, which is formally very similar and reduces to the usual Born and Born-Markov master equations at sufficiently weak coupling, but has a “self-consistent” dissipator allowing to capture stronger-coupling regimes at a little extra numerical cost. Furthermore, we discuss how the NCA maps can be benchmarked evaluating the leading-order self-consistent correction, the one crossing approximation (OCA).

We then apply the NCA and NCA-Markov maps to the spin-boson model with a zero temperature environment. We show that in the case of a Ohmic environment both approaches correctly capture the non-perturbative dynamics of this model at strong system-bath coupling, including its crossover from coherent to incoherent dynamics and its quantum phase transition to a localized phase, which are completely missed by the Born and Born-Markov master equations. Finally, computing the one-crossing correction to NCA we show for both a Ohmic and a sub-Ohmic environment that these approaches are quantitatively accurate in weak-coupling regimes in which the latter master equations already display significant deviations.

2 From master equations to dynamical maps

We consider a generic quantum system coupled to a bath with total Hamiltonian $H_{\text{tot}} = H_S + H_B + H_{SB}$, where H_S and H_B are respectively the system and bath Hamiltonians and where the system-bath coupling can be generically written as $H_{SB} = \sum_k X_k \otimes B_k$, with $X_k = X_k^\dagger$ and $B_k = B_k^\dagger$ respectively system and bath operators.

To simplify the notation we consider a single coupling to the bath $H_{SB} = X \otimes B$ but our approach trivially extends to multiple couplings. We also assume that the bath is described by a set of non-interacting bosonic modes with annihilation operators a_i corresponding to $H_B = \sum_i \omega_i a_i^\dagger a_i$ and we take $B = \sum_i \frac{\lambda_i}{2} (a_i + a_i^\dagger)$, where λ_i is the strength of the coupling with the bath modes. Finally, we consider a factorized system-bath density matrix at time $t = 0$, $\rho_{\text{tot}}(0) = \rho(0) \otimes \rho_B(0)$, and an initial bath density matrix $\rho_B(0)$ that is stationary with respect to H_B .

Under those assumptions, the reduced dynamics of the system is often conveniently described by master equations of the form [98]

$$\partial_t \rho(t) = \hat{\mathcal{H}}_S \rho(t) + \int_0^t dt_1 \hat{\mathcal{D}}(t - t_1) \rho(t_1) \quad (1)$$

where $\hat{\mathcal{D}}$ is the dissipator, describing the influence of the bath on the system. Weak-coupling master equations are based on a second-order approximation in the system-bath coupling, the Born approximation [98], that leads to the dissipator

$$\hat{\mathcal{D}}_{\text{Born}}(\tau) = \Gamma(\tau) \left(e^{\hat{\mathcal{H}}_s \tau} [X \bullet] X - X e^{\hat{\mathcal{H}}_s \tau} X \bullet \right) + \text{H.c} \quad (2)$$

in which the superoperator $\hat{\mathcal{H}}_s \bullet = -i[H_S, \bullet]$ describes the bare system dynamics and where Γ is the bath correlation function

$$\Gamma(\tau) = \text{tr}[B(\tau)B(0)\rho_B(0)] \quad (3)$$

with $B(\tau)$ time-evolved with the bath Hamiltonian H_B . We used square brackets in (2) when necessary to indicate the argument of superoperators. The dissipator (2) has the familiar structure of Redfield [2] and Lindblad [28] master equations, as the Born master equation defined by (1) and (2) is the starting point for deriving them.

Heuristically, we introduce the NCA self-consistent map in two steps: by first recognizing that the dynamical map $\hat{\mathcal{V}}(t)$, namely the superoperator evolving the system density matrix from the initial state, $\rho(t) = \hat{\mathcal{V}}(t)\rho(0)$, obeys the same equation

$$\partial_t \hat{\mathcal{V}}(t) = \hat{\mathcal{H}}_s \hat{\mathcal{V}}(t) + \int_0^t dt_1 \hat{\mathcal{D}}(t-t_1) \hat{\mathcal{V}}(t_1) \quad (4)$$

Then, we make the Born dissipator self-consistent by replacing in (2) the evolution superoperator $e^{\hat{\mathcal{H}}_s \tau}$, describing the dynamics of the system isolated from the environment, with the dynamical map $\hat{\mathcal{V}}(\tau)$ itself, taking into account the influence of the environment:

$$\hat{\mathcal{D}}_{\text{NCA}}(\tau) = \Gamma(\tau) \left(\hat{\mathcal{V}}(\tau) [X \bullet] X - X \hat{\mathcal{V}}(\tau) X \bullet \right) + \text{H.c} \quad (5)$$

where for taking the Hermitian conjugate one can use the property $(\hat{\mathcal{V}}[\bullet])^\dagger = \hat{\mathcal{V}}[\bullet^\dagger]$. Eq. (4) with the dissipator (5) has a very similar structure to standard master equations, but is an equation for the dynamical map rather than for the density matrix. Its solution is the NCA dynamical map. Differently from standard master equations, the dissipator (5) is determined “self-consistently” as it depends on the unknown.

Apart from this heuristic derivation, a formal derivation using diagrammatic techniques is given in App. E, where (4) is recognized as the Dyson equation for the perturbation theory of the dynamical map $\hat{\mathcal{V}}(t)$ in the system-bath coupling and the dissipator $\hat{\mathcal{D}}$ as its self-energy (the same is true for Eq. (1) and $\rho(t)$). An important consequence is that (4) (as (1)) is in principle an exact equation, where the exact self-energy $\hat{\mathcal{D}}$ is defined by its perturbation series. A diagrammatic representation of this series along with the approximations schemes considered in this manuscript is shown in Fig. 1: a lowest-order truncation of the series corresponds to the Born approximation (2), while approximating it with the sum of its infinitely-many “non-crossing” diagrams (hence the name NCA) yields the simple analytic expression in terms of $\hat{\mathcal{V}}(t)$ in Eq. (5).

The NCA map is non-perturbative as its dissipator (5) includes contributions to all orders in the bath correlation function Γ (or in the system-bath coupling H_{SB}), in contrast with the Born dissipator (2) which is first order in Γ (2nd order in H_{SB}). To see this explicitly, one can obtain $\hat{\mathcal{V}}$ by integrating Eq. (4), and plug it in Eq. (5) to get an expression for the dissipator which explicitly depends on Γ , Γ^2 and $\hat{\mathcal{V}}$: substituting $\hat{\mathcal{V}}$ recursively, contributions up to all powers in Γ are generated. This allows the NCA map to capture stronger coupling effects with respect to standard master equations based on the Born approximation, like Redfield [2] and Lindblad-Davies equations [27]. We also remark that, when the coupling is sufficiently weak the NCA maps

$$\begin{aligned}
 \widehat{\mathcal{D}} &= \overset{\text{NC}}{\text{---}} + \overset{\text{NC}}{\text{---}} + \overset{\text{NC}}{\text{---}} + \text{---} + \dots \\
 \widehat{\mathcal{D}}_{\text{Born}} &= \text{---} \\
 \widehat{\mathcal{D}}_{\text{NCA}} &= \text{---} \quad \widehat{\mathcal{D}}_{\text{OCA}} = \text{---} + \text{---}
 \end{aligned}$$

Figure 1: The expression at the top represents the (first terms of the) exact series for the dissipator $\widehat{\mathcal{D}}$ which is the self-energy of the Dyson equation (4): non-bold solid lines represent bare evolution superoperators $e^{\hat{\mathcal{H}}_s(\tau)}$, dashed lines correspond to bath correlation functions (3), with a typical decay time τ_b . The middle expression shows that retaining the 1st term of the series corresponds to the Born dissipator (2). At the bottom, the NCA dissipator (5) corresponds to the sum of all the diagrams in which the dashed lines do not cross (labelled by “NC”), which can be expressed in terms of a bold solid line representing the dynamical map $\hat{\mathcal{V}}$. Similarly, $\widehat{\mathcal{D}}_{\text{OCA}}$ is the dissipator including the leading-order self-consistent correction to NCA, namely in the one-crossing approximation (OCA). We also show that $\widehat{\mathcal{D}}_{\text{OCA}}$ decays on a longer time-scale $2\tau_b$ than $\widehat{\mathcal{D}}_{\text{NCA}}$, decaying in τ_b .

become equivalent to standard weak-coupling master equations, as to lowest order in the system-bath coupling the NCA dissipator (5) reduces to the Born one (2): $\hat{\mathcal{V}}(\tau)$ in (5) reduces to $e^{\hat{\mathcal{H}}_s\tau}$.

A more extended discussion of the regime of validity of the NCA maps and on how to benchmark their predictions introducing the leading-order self-consistent corrections is reported in Section 2.2. In the following Section we show how the usual Markovian approximation done for master equations can be combined with the NCA, while other points in common with those equations are the steady-state equation reported in C and a quantum regression theorem for computing correlation functions in G.1. The main equations for a coupling in the rotating-wave approximation are also reported in Appendix B (see also [97]).

2.1 Markovian approximation

When the bath-induced dynamics on the system is slower than the typical decay time of the dissipator, one can do a Markovian approximation of replacing $\hat{\mathcal{V}}(t_1)$ in (4) with $e^{\hat{\mathcal{H}}_s(t_1-t)}\hat{\mathcal{V}}(t)$, yielding the time-local equation:

$$\partial_t \hat{\mathcal{V}}(t) = \left[\hat{\mathcal{H}}_s + \int_0^t d\tau \hat{\mathcal{D}}(\tau) e^{-\hat{\mathcal{H}}_s(\tau)} \right] \hat{\mathcal{V}}(t) \quad (6)$$

Combining the Markovian approximation (6) with the non-crossing approximation (5) yields the NCA-Markov dynamical map. The validity of combining these approximations is discussed in Appendix E.4.

The same Markovian approximation is routinely done at the level of master equations (1), where $\rho(t_1)$ is replaced with $e^{\hat{\mathcal{H}}_s(t_1-t)}\rho(t)$, leading to the Born-Markov master equation, that we report explicitly and connect to its standard form in Appendix F. Since we will use the Born-Markov master equation for comparison later, we remark that, despite the name, we keep the integration

time in (1) finite, rather than extending it to infinity as one would do to obtain a fully Markovian master equation.

2.2 Validity of NCA and benchmarking with higher-order self-consistent schemes

The NCA maps can be generalized to a whole hierarchy of self-consistent approximations, where the dissipators always depend on $\hat{\mathcal{V}}$ rather than on $e^{\hat{\mathcal{H}}_s\tau}$. This is achieved using standard results of many-body theory that allow to rewrite self-energies in terms of “bold” or “skeleton” diagrams [99]. Each approximation in the hierarchy has contributions up to all powers in the system-bath coupling in the dissipator, still the hierarchy is ordered, such that higher-order terms become negligible for a sufficiently small system-bath coupling. The NCA corresponds to lowest order approximation of the hierarchy.

The NCA maps therefore become quantitatively correct when the coupling with the environment is sufficiently weak, such that the higher-order self-consistent corrections become negligible. We remark that they might still be quantitatively accurate in regimes in which Born-based master equations already show significant deviations from the correct solution, as we demonstrate for the spin-boson model in Sec. 3.2. Given their non-perturbative nature, the NCA maps might also be able to capture qualitatively the physics in the strong-coupling regime, while quantitative accuracy cannot be expected there, as we show in section G.1.

The natural strategy to assess the validity of the results of the NCA maps is to evaluate the leading-order self-consistent correction. This is known as “one-crossing approximation” (OCA) (see e.g. [91, 100]) and still has a compact expression adding one term to the NCA dissipator, that we derive and report in Appendix E.5. We compute and discuss the OCA corrections for the spin-boson model in Sec. 3.2.

We also remark that the NCA maps exactly preserve trace and Hermiticity of the density matrix [97].

Finally, we remark that the decay time τ_b of the bath correlation function $\Gamma(\tau)$ is the shortest timescale for system-bath interactions in standard master equations [33, 98, 101–103], while the NCA maps capture processes that happen on faster scales. Also, for both NCA and Born approximations, τ_b is the decay time of the dissipator and therefore the timescale over which Eq. (4) loses its “memory” of the past. Upon including higher-order self-consistent diagrams, the decay-time of the dissipator and thus the memory allowed by these approximations systematically increases; this is also shown in Fig. 1.

2.3 Numerical implementation and cost

With respect to standard master equations based on the Born approximation (1), equation (4) for the dynamical map is a non-linear integro-differential equation. Non-linear equations can in principle lead to numerical instabilities, as for example one might encounter discretizing Eq. (4) with the simplest, explicit Euler scheme. On the other hand, Eq. (4) has the form of a Dyson equation with a self-consistent self-energy, which is often encountered in many-body physics and for which several stable discretization schemes are known (see e.g. [104] and references therein). Here we use a simple and efficient implicit second-order Runge-Kutta scheme adapted from Ref. [104] and described in Appendix A, which is found to be numerically very stable (also in the case of a larger Hilbert space [105]).

The key advantage of the NCA maps over standard master equations based on the Born approximation is that they can capture stronger coupling regimes with a little extra numerical cost

and with a similar formalism. The NCA map has a computational cost for time-propagation which is $O(t^2)$, like the Born master equation, and the NCA-Markov map has cost $O(t)$, as Redfield [2] or Lindblad equations [98]. The main computational disadvantage with respect to master equations is dealing with $\hat{\mathcal{V}}$ which has size N^4 , where N is the size of the system Hilbert space, instead of with ρ having size N^2 . While this is certainly not an issue for systems with a small Hilbert space, for larger systems these approaches might still be much cheaper than exact non-perturbative methods, and therefore might also be advantageous in combination with already numerically demanding many-body approaches [105, 106].

3 Application to the spin-boson model

In the following, we demonstrate the NCA and NCA-Markov dynamical maps on the spin-boson model and compare them to the Born and Born-Markov master equations.

This model describes a quantum spin 1/2 with tunneling strength Δ coupled to a bosonic bath with Hamiltonian

$$H = \frac{\Delta}{2}\sigma^x + \frac{\lambda}{2}\sigma^z \sum_i (a_i^\dagger + a_i) + \sum_i \omega_i a_i^\dagger a_i \quad (7)$$

Despite its simple Hamiltonian, the spin boson model has a non-trivial physics that has been previously investigated with many theoretical methods [67, 107–126]. It can also be nowadays realized in several experimental setups [24, 48, 54]. Identifying $X = \sigma^z$ and $B = \frac{\lambda}{2} \sum_i (a_i^\dagger + a_i)$, then the bath correlation function $\Gamma(t)$ (3), is fixed by specifying the density of states of the bath modes and its temperature. We consider here a zero temperature bath for which

$$\Gamma(\tau) = \int_0^\infty \frac{d\xi}{2\pi} J(\xi) \frac{1}{2} (\cos(\xi t) - i \sin(\xi t)) \quad (8)$$

and the bath density of states is taken of the form

$J(\omega) = \sum_i \pi \lambda^2 \delta(\omega - \omega_i) = 2\pi \alpha \omega_c^{1-s} \omega^s \theta(\omega) \theta(\omega_c - \omega)$, with a sharp cutoff ω_c and where α is the dimensionless system-bath coupling strength $\alpha = \lambda^2 / (2\omega_c^2)$ (we fix $\omega_c = 1$ and $\Delta/\omega_c = 0.1$ throughout the manuscript). For $s = 1$ this corresponds to a Ohmic environment and for $s < 1$ to a sub-Ohmic one, that will be considered in the following.

3.1 Ohmic spin-boson at strong coupling

The Ohmic spin boson physics ($s = 1$) in the limit $\Delta \ll \omega_c$ is well understood already from the seminal work [110]: for $\alpha < 1/2$, there are coherent oscillations (tunneling) between the σ^z eigenstates at a renormalized spin frequency Δ_r which are damped by the environment, for $\alpha > 1/2$ then Δ_r is still finite but oscillations are overdamped and the dynamics is incoherent, while for $\alpha > \alpha_c = 1$ tunneling is suppressed and the spin enters a localized phase with $\Delta_r = 0$, through a quantum-phase transition.

Fig. 2 shows the transient dynamics of the system starting from $\rho(0) = |\downarrow\rangle\langle\downarrow|$, with $\sigma^z |\downarrow\rangle = -1 |\downarrow\rangle$. The spin-boson physics discussed above is captured both by the NCA and NCA-Markov maps, as shown in the left-bottom panel plotting the dynamics of $\langle\sigma_z\rangle$. They capture a crossover between a coherent spin dynamics for $\alpha < \alpha_{\text{cross}}$, characterized by underdamped oscillations, and an incoherent dynamics for $\alpha > \alpha_{\text{cross}}$ where oscillations are overdamped. Numerically we locate the crossover at $\alpha_{\text{cross}} \sim 0.2$, a quantitative discrepancy with respect to more accurate estimates [110].

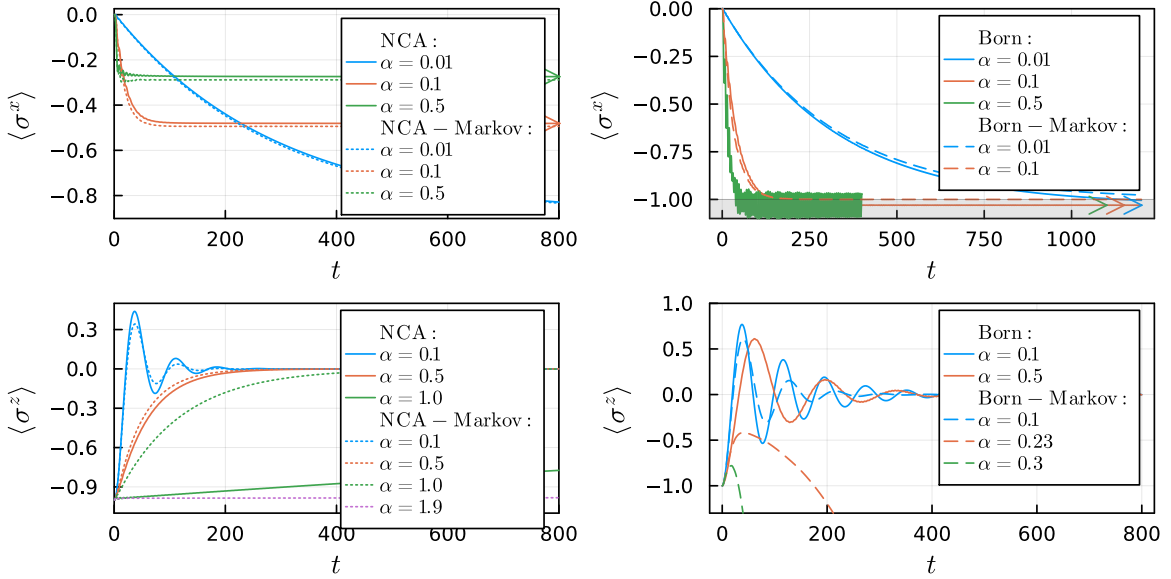


Figure 2: Dynamics of the spin boson model, for $\Delta/\omega_c = 0.1$, $\omega_c = 1$, computed with the NCA and NCA-Markov maps (left column) and with the Born and Born-Markov master equations (right column) for different values of the system-bath coupling α , starting from $\rho(0) = |\downarrow\rangle\langle\downarrow|$. The top panels show the relaxation of $\langle\sigma^x\rangle$ to its stationary value (indicated with arrows for NCA and Born). The NCA approaches predict a non-trivial dependence of the steady-state on the system-bath coupling, which is missing in Born and Born-Markov, even for small couplings. The bottom panels show the dynamics of $\langle\sigma^z\rangle$. The NCA approaches (bottom-left) capture a loss of spin coherence for $\alpha > \alpha_{\text{cross}} \sim 0.2$. Also, they predict that the timescale for $\langle\sigma^z\rangle$ relaxation grows as α approaches a critical value α_c , signaling the onset of the spin-boson delocalization transition. These features are not captured by the Born-based master equations (bottom-right). The right panels show the breakdown of the Born approximation, developing unphysical oscillations, and of the Born-Markov one, developing an unphysical instability. The time-step used is $dt = 0.1 \times 2\pi/\omega_c$, apart for the Born dynamics where $dt = 0.01 \times 2\pi/\omega_c$.

We also note that in this regime the NCA and NCA-Markov agree remarkably well and that memory effects do not seem to play a major role. Increasing the system-bath coupling, we see that both NCA and NCA-Markov approaches predict a growth of the spin relaxation timescale as α approaches the critical value, which witnesses the onset of the localization quantum phase transition [113]. While the qualitative behaviour of the two theories is similar, the NCA approach predicts $\alpha_c \approx 1$, as expected [110], while NCA-Markov predicts a critical point at $\alpha_c \approx 1.9$. The renormalization of the spin frequency down to zero at the localization transition can be equally inferred from the stationary-state correlation functions that we report in Appendix G.1.

On the other hand, the Born-based master equations fail to reproduce, even qualitatively, the crossover to an incoherent regime and the localization transition (bottom-right panel) characterizing the spin boson model. The Born-Markov approximation is numerically divergent for $\alpha \simeq 0.23$, while the Born one, despite not diverging, never predicts a crossover to over-damped oscillations (see bottom-right panel, but we also checked much larger values up to $\alpha \sim 100$). That the Born-based master equations cannot predict the localization transition is also evident from the analysis

of steady-state correlation functions in Appendix G.1.

Remarkably instead, the NCA maps can qualitatively capture the strong-coupling physics of the model, which is particularly remarkable for the NCA-Markov map as for a Ohmic bath at zero temperature the dynamics is not a priori expected to be Markovian [30], but it can indeed become effectively Markovian [127–130].

The upper panels show instead the relaxation of $\langle \sigma_x \rangle$ to its stationary value (indicated by arrows), for different values of α . For a vanishingly small system-bath coupling the spin thermalizes to its ground state, where $\langle \sigma^x \rangle = -1$, while increasing α the coupling with the bath drives the spin towards the z direction, and thus $\langle \sigma^x \rangle$ decreases. We remark that the NCA maps reproduce the expected behaviour in the whole delocalized phase (top left panel).

Instead, the Born and Born-Markov master equations cannot capture any steady-state dependence on α (see Appendix G.3), and thus they cannot predict the $\langle \sigma^x \rangle$ dynamics correctly (top-right panel). Similar pathologies are known to severely limit these equations, even at small couplings [131, 132]. We also note that the Born master equation develops unphysical $\langle \sigma_x \rangle$ oscillations (top-right panel), reminiscent of an unphysical gap in the equilibrium σ_x correlation functions [124], and unphysical < 1 steady-state values of this quantity.

Finally, for α larger than the critical value, we find (not shown) that both the NCA and NCA-Markov approaches become unstable, yielding density matrices with negative probabilities. This instability of the NCA approaches, though, only arises in correspondence of the localization transition, likely because the NCA approximation cannot capture the spontaneous development of finite coherences in the bath $\langle B \rangle \neq 0$ in the localized phase. We emphasize however that within the entire delocalized phase the NCA maps never showed the tendency to develop non-positive density matrices, while the Born master equation did (see top-right panel).

In addition, to further highlight the ability of the NCA map to go beyond standard master equations, in Appendix G.1 we computed the steady-state correlation functions showing how the spin transition frequency is renormalized to zero at the localization transition in NCA, while this never happens for Born-based master equations. In Appendix G.2 we studied the response of the spin-boson model with a finite bias and shown that it reproduces the crossover to an incoherent regime observed experimentally in [48] that Born-based master equations fail at predicting.

3.2 Ohmic and sub-Ohmic dynamics at weak coupling

Here we evaluate the leading-order self-consistent correction to NCA, called one-crossing approximation (OCA) (38), to test the NCA maps predictions for a spin-boson model with both a Ohmic and sub-Ohmic environment. Fig. 3 shows a comparison between NCA, OCA and the Born approximation, showing that, in the weak coupling regime considered here, NCA yields quantitatively accurate predictions, as the OCA corrections are negligible. At the same time, the Born approximation shows significant deviations in this regime, demonstrating the advantage of the NCA-maps.

In particular, in the top panel we consider the short-time dynamics of $\langle \sigma_x \rangle$ for the Ohmic spin-boson model ($s = 1$). The Born approximation shows significant deviations already for very small couplings, because it always predicts a steady state value $\langle \sigma_x \rangle(t \rightarrow \infty) = -1$, as we discussed earlier.

In the bottom panel we consider instead a sub-Ohmic spin-boson model ($s < 1$), as for this model the localization transition happens for smaller values of the system-bath coupling [124], influencing more strongly the weak coupling dynamics, where a quantitative comparison between the NCA, OCA and Born approximations is possible. The bottom panel of Fig. 3 for $s = 0.4$ shows that the NCA predictions for the dynamics of $\langle \sigma_z \rangle$ agree with the OCA ones, while the Born ap-

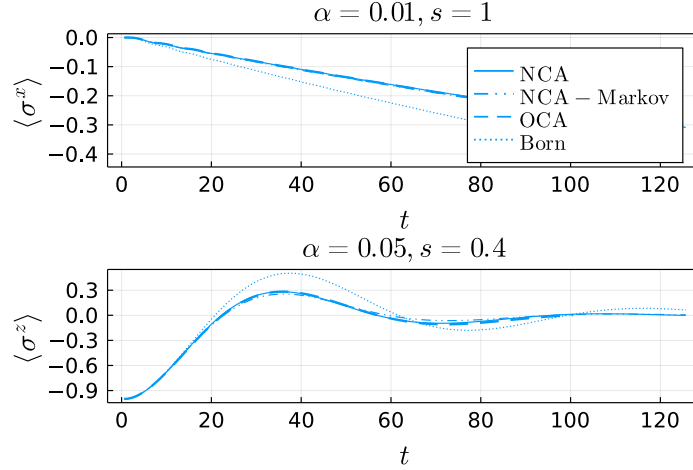


Figure 3: A comparison between NCA, OCA and the Born approximation. The NCA predictions are shown to be quantitatively correct for these sets of parameters, since the OCA predictions are on top of the NCA ones. The Born master equation shows instead significant deviations. The top panel shows the dynamics of $\langle \sigma_x \rangle$ for the Ohmic spin-boson model considered in the main text. The bottom panel shows the dynamics of $\langle \sigma_z \rangle$ a sub-Ohmic spin-boson model with $s = 0.4$. The levels splitting and bath cutoff are $\Delta/\omega_c = 0.1, \omega_c = 1$.

proximation shows significant deviations. Differently from the top panel, all the methods yield the same steady state value for $\langle \sigma_z \rangle$, thus the differences in the predictions of the different methods are purely dynamical.

We also remark that the NCA-Markov approach in Fig. 3 is also in good agreement with NCA and OCA predictions, showing that the Born approximation is much more limiting than the Markovian approximation here.

Finally, we remark that for the Ohmic spin-boson model at stronger system-bath coupling the OCA predictions are qualitatively similar to NCA ones, predicting a crossover to incoherent dynamics and a localization transition (not shown), but no quantitative agreement has to be expected in this strong-coupling regime.

4 Conclusion

In this work we have introduced the NCA and NCA-Markov maps dynamical maps for open quantum systems. These approaches are formally very similar to conventional master equations based on the Born and Born-Markov approximation and become equivalent to them in the weak-coupling limit, but can also capture stronger coupling effects at very little extra numerical cost and therefore might be preferred in several numerical studies of open quantum systems. We have also discussed how the NCA maps can be benchmarked evaluating the leading order self-consistent correction, the one-crossing approximation (OCA).

We applied the NCA maps to the spin-boson model at zero temperature, showing how they qualitatively capture its strong-coupling physics in presence of a Ohmic bath, including its crossover between coherent and incoherent dynamics and its phase transition towards a localized phase, sig-

nalled by a growth of the spin relaxation time-scale and a renormalization of the spin frequency to zero, which conventional weak-coupling master equations fail at predicting. We have also evaluated the leading-order OCA correction both for a Ohmic and a sub-Ohmic spin-boson model, showing that the NCA maps also yield quantitatively correct predictions in a weak-coupling regime in which standard master equations show significant deviations.

We expect the NCA maps to find a variety of applications beyond the model considered in this paper, including electronic transport problems where standard master equations are not sufficient to account for lifetime broadening effects [39–41], driven problems where other approaches show limitations [48], quantum emitters coupled to nanophotonic structures where non-perturbative regimes arise [133–135], or to be embedded in many-body approaches for lattice models [53, 105, 106].

Acknowledgements

Funding information We acknowledge computational resources on the Collège de France IPH cluster. This work was supported by the ANR grant "NonEquMat" (ANR-19-CE47-0001).

A Implementation of a 2nd order Runge-Kutta scheme

Equation (4) is a Volterra integral-differential equation, that often appears in many-body problems, with the form

$$\frac{d}{dt}y(t) = q(t) + p(t)y(t) + \int_0^t d\bar{t}k(t, \bar{t})y(\bar{t}) \quad (9)$$

where in our case of an equilibrium bath the memory kernel depends only on time differences. Several stable discretization schemes can be used to solve it and here we implemented a 2nd order Runge-Kutta scheme adapted from [104], Appendix A, to propagate it in time.

In the present case we adapt that scheme, such as to capture correctly the case in which the memory kernel has a $\delta(t)$ contribution, for example in the case of a Markovian environment. By integrating (9) up to the time-steps t_n and t_{n-1} and subtracting the two equations, we get

$$y(t_n) - y(t_{n-1}) = \Delta t \sum_{i=0}^{n-1} (w_{n,i} - w_{n-1,i}) y'(t_i) + \Delta t w_{n,n} y'(t_n) \quad (10)$$

which is Eq. A5 of [104], with $w_{n,i}$ ($i = (0, 1, \dots, n)$) some weights that depend on the scheme chosen for approximating integrals (Euler, trapezoids, Simpson's rule, ecc). $y'(t_n)$ is then evaluated by discretizing (9). In doing so, we allow $k(t, \bar{t})$ to have a $\delta(t - \bar{t})$ contribution. To correctly take it into account, we discretize the integral as

$$\begin{aligned} \int_0^{t_n} d\bar{t}k(t_n, \bar{t})y(\bar{t}) &= \int_0^{t_{n-1}} d\bar{t}k(t_n, \bar{t})y(\bar{t}) + \int_{t_{n-1}}^{t_n} d\bar{t}k(t_n, \bar{t})y(\bar{t}) = \\ &= \Delta t \sum_{i=0}^{n-1} w_{n-1,i} k(t_n, t_i) y(t_i) + \Delta t k(t_n, t_n) y(t_n) \end{aligned} \quad (11)$$

where we discretized the last time-step separately, to make sure that $k(t_n, t_n)$ is evaluated with weight 1, such as to fully capture a $\delta(t - \bar{t})$ contribution (instead of discretizing the whole integral with a single scheme).

In our implementation, we use a second-order Runge-Kutta scheme for the weights $w_{n,i}$, corresponding to

$$w_{n,i} = \begin{cases} 1/2 & i = 0, n \\ 1 & 1 \leq i \leq n-1 \end{cases} \quad (12)$$

leading to

$$\begin{aligned} y'(t_n) &= q(t_n) + p(t_n)y(t_n) + \Delta t k(t_n, t_n)y(t_n) + \\ &\frac{\Delta t}{2} [k(t_n, t_0)y(t_0) + k(t_n, t_{n-1})y(t_{n-1})] + \Delta t \sum_{i=1}^{n-2} k(t_n, t_i)y(t_i) \end{aligned} \quad (13)$$

$$y(t_n) - y(t_{n-1}) = \frac{\Delta t}{2} [y'(t_{n-1}) + y'(t_n)] \quad (14)$$

Using those equations it is possible to determine $y(t_n), y'(t_n)$, given their values for $t_{n'} < t_n$ and an initial condition for $y(t_0), y'(t_0)$ (in our case $\hat{Y}(0) = \mathbb{1}$ and $\partial_t \hat{Y}(0)$ is given by Eq. (4)). If $k(t, \bar{t})$ doesn't depend on y one might eliminate $y'(t_n)$ and find a closed equation for $y(t_n)$. Since in our case $k(t, \bar{t})$ depends on y as well, we iterate the 2 equations above to find $y(t_n), y'(t_n)$.

B System-bath coupling in the Rotating Wave Approximation

Here we consider the case of a system-bath coupling in the form $\hat{H}_{SB} = \tilde{X} \otimes \tilde{B}^\dagger + \tilde{X}^\dagger \otimes \tilde{B}$, which is common when performing a rotating-wave approximation. Here $\tilde{B} = \sum_i \frac{\tilde{\lambda}_i}{2} a_i$. In this case the NCA dissipator is given by

$$\begin{aligned} \hat{\mathcal{D}}(\tau) = & \tilde{\Gamma}^<(\tau) (\tilde{X}^\dagger \hat{\nu}(\tau) [\bullet] \tilde{X} - \hat{\nu}(\tau) [\bullet \tilde{X}] \tilde{X}^\dagger) + \\ & \tilde{\Gamma}^>(\tau) (\hat{\nu}(\tau) [\tilde{X} \bullet] \tilde{X}^\dagger - \tilde{X}^\dagger \hat{\nu}(\tau) [\tilde{X} \bullet]) + \text{H.c} \end{aligned} \quad (15)$$

with $\tilde{\Gamma}^>(\tau) = \text{tr}[\tilde{B}(\tau)\tilde{B}^\dagger(0)\rho_B(0)]$ and $\tilde{\Gamma}^<(\tau) = \text{tr}[\tilde{B}^\dagger(\tau)\tilde{B}(0)\rho_B(0)]$.

In this case, the correlation functions take the form

$$\begin{aligned} \langle \tilde{X}(t)\tilde{X}^\dagger(t') \rangle &= \text{tr}[\tilde{X}\hat{\nu}(t,t')\tilde{X}^\dagger\rho(t')] \theta(t-t') \\ &+ \text{tr}\{\tilde{X}^\dagger\hat{\nu}(t',t)[\rho(t)\tilde{X}]\} \theta(t'-t) \\ \langle \tilde{X}^\dagger(t)\tilde{X}(t') \rangle &= \text{tr}[\tilde{X}^\dagger\hat{\nu}(t,t')\tilde{X}\rho(t')] \theta(t-t') \\ &+ \text{tr}\{\tilde{X}\hat{\nu}(t',t)[\rho(t)\tilde{X}^\dagger]\} \theta(t'-t) \end{aligned} \quad (16)$$

C Steady-state equation

Assuming that the system forgets its initial conditions at a sufficiently long time and reaches a time-independent steady-state, defined as $\rho_s = \lim_{t \rightarrow \infty} \hat{\nu}(t,0)\rho(0)$, this state also obeys the equation [97, 105]

$$\left(\hat{\mathcal{H}}_s + \int_0^\infty d\tau \hat{\mathcal{D}}(\tau) \right) \rho_s = 0 \quad (17)$$

We remark that at weak system-bath coupling $\hat{\mathcal{D}}(\tau)$ is expected to decay on a shorter timescale than that for the system to reach the steady-state. Eq. (17) then allows to extract ρ_s from the short-time dynamics of the system, akin to the condition for finding the steady-states of Markovian master equations in terms of the generator of their infinitesimal time-evolution, the Liouvillian.

D Steady state correlation functions

The *quantum regression theorem* for Markovian master equations allows to compute (multi-time) correlation functions from the same generator of the dynamics which evolves the density matrix [98]. This result is generalized in NCA [97, 105], at least for the two-times correlation functions of the operator X which couple to the bath, which can be computed from the formula

$$\begin{aligned} \langle X(t)X(t') \rangle &= \text{tr}[X\hat{\nu}(t-t')X\rho(t')] \theta(t-t') \\ &+ \text{tr}\{X\hat{\nu}(t'-t)[\rho(t)X]\} \theta(t'-t) \end{aligned} \quad (18)$$

Note that $\langle X(t)X(t') \rangle = \langle X(t')X(t) \rangle^*$ relates the $t > t'$ with the $t < t'$ expression. We remark that a similar result is not expected to hold for generic non-Markovian approaches and it is a peculiar property of NCA.

E Formal derivation of the self-consistent dynamical maps

E.1 Perturbation theory in the system-bath coupling

In this section we derive the perturbation series for the evolution superoperator in the system-bath coupling, up to all orders in this coupling. This leads to the Dyson equation (4) of the main text and sets the stage for developing the non-crossing approximation.

We recall that the evolution superoperator $\hat{\mathcal{V}}$ is defined by $\rho(t) = \text{tr}_B \rho_{\text{tot}}(t) = \hat{\mathcal{V}}(t)\rho(0)$ where $\rho_{\text{tot}}(t) = e^{-iHt}\rho_{\text{tot}}(0)e^{iHt}$ and the total Hamiltonian is given by $H = H_S + H_B + H_{SB}$ and where tr_B is a partial trace on bath operators. By moving to the interaction picture, the following identities can be found for the evolution operators

$$e^{-iHt} = e^{-i(H_S+H_B)t} T_t e^{-i \int_0^t dt' H_{SB}(t')} = e^{-i(H_S+H_B)t} T_t \sum_{n=0}^{\infty} \frac{(-i)^n}{n!} \left[\int_0^t dt' H_{SB}(t') \right]^n \quad (19)$$

$$e^{iHt} = \check{T}_t e^{i \int_0^t dt' H_{SB}(t')} e^{i(H_S+H_B)t} = \check{T}_t \sum_{n=0}^{\infty} \frac{(+i)^n}{n!} \left[\int_0^t dt' H_{SB}(t') \right]^n e^{i(H_S+H_B)t} \quad (20)$$

Here $H_{SB}(t') = e^{i(H_S+H_B)t'} H_{SB} e^{-i(H_S+H_B)t'}$ and T_t is the real-time time-ordering operator. The latter takes any product of operators, where each operator is defined at one time, and changes the order so that every operator has only later operators to the left and earlier operators to the right. For non-fermionic variables as those we will consider, this change of order doesn't introduce any sign. The anti-time-ordering operator \check{T}_t instead enforces the opposite ordering. Plugging in these expressions and using the cyclic property of the partial trace on the bath, one finds

$$\hat{\mathcal{V}}(t)\rho(0) = e^{-iH_S t} \text{tr}_B \left\{ T_t \sum_{k_+=0}^{\infty} \frac{(-i)^{k_+}}{k_+!} \left[\int_0^t dt' H_{SB}(t') \right]^{k_+} \rho_{\text{tot}}(0) \check{T}_t \sum_{k_-=0}^{\infty} \frac{(+i)^{k_-}}{k_-!} \left[\int_0^t dt' H_{SB}(t') \right]^{k_-} \right\} e^{iH_S t} \quad (21)$$

In order to manage this double series expansion, it is convenient to use the superoperators notation already introduced in the main text. We define

$$\hat{H}_{SB\gamma}(t') \bullet = \begin{cases} H_{SB}(t') \bullet & \text{if } \gamma = + \\ \bullet H_{SB}(t') & \text{if } \gamma = - \end{cases} \quad (22)$$

Using this definition, we note that the time-ordering structure of the operators in Eq. (21), that are time-ordered on the left of the density matrix and anti-time-ordered on its right, is obtained in the superoperator notation if superoperators with $\gamma = +$ and $\gamma = -$ are time-ordered separately, putting superoperators with later times on the left regardless of their index γ (instead of those with $\gamma = -$ being anti-time-ordered). We therefore introduce the operator T_C enforcing this time-ordering of a string of superoperators (the notation recalls that of the contour-time-ordering operator in Keldysh field theory, which is analogous). This is easily understood with an example. Suppose $t_1 > t_2 > t_3 > t_4$, then

$$\begin{aligned} T_C \hat{O}_-(t_3) \hat{O}_-(t_4) \hat{O}_+(t_1) \hat{O}_+(t_2) \bullet &= \hat{O}_-(t_3) \hat{O}_-(t_4) \hat{O}_+(t_1) \hat{O}_+(t_2) \bullet = \\ &= O(t_1) O(t_2) \bullet O(t_4) O(t_3) = T_t O(t_1) O(t_2) \bullet \check{T}_t O(t_3) O(t_4) \end{aligned} \quad (23)$$

We also note that superoperators with different γ indexes commute by definition, $\hat{O}_+(t_1) \hat{O}_-(t_2) \bullet = \hat{O}_-(t_2) \hat{O}_+(t_1) \bullet = O(t_1) \bullet O(t_2)$, thus we can always assume that a string of

superoperators under T_C is time-ordered according to their real-time variable, regardless of their indexes γ . Using the previous example

$$\begin{aligned} T_C \hat{O}_-(t_3) \hat{O}_-(t_4) \hat{O}_+(t_1) \hat{O}_+(t_2) &= \hat{O}_-(t_3) \hat{O}_-(t_4) \hat{O}_+(t_1) \hat{O}_+(t_2) = \\ &= \hat{O}_+(t_1) \hat{O}_+(t_2) \hat{O}_-(t_3) \hat{O}_-(t_4) \end{aligned} \quad (24)$$

where in the last equality the superoperators are ordered according to their real time variables $t_1 > t_2 > t_3 > t_4$. We also define the bare evolution superoperator $\hat{\mathcal{V}}_0(t) = e^{-iH_S t} \bullet e^{iH_S t}$. With these definitions one can write

$$\hat{\mathcal{V}}(t)\rho(0) = \hat{\mathcal{V}}_0(t)\text{tr}_B \left\{ T_C \sum_{k_+, k_- = 0}^{\infty} \frac{(-i)^{k_+ + k_-}}{k_+! k_-!} \left[\int_0^t dt' \hat{H}_{SB+}(t') \right]^{k_+} \left[- \int_0^t dt' \hat{H}_{SB-}(t') \right]^{k_-} \rho_{\text{tot}}(0) \right\} \quad (25)$$

By doing some combinatorial calculations, it's easy to show that the double summation can be reduced to a single one and that the following identity is valid:

$$\hat{\mathcal{V}}(t)\rho(0) = \hat{\mathcal{V}}_0(t)\text{tr}_B \left\{ T_C e^{-i \int_0^t dt' \sum_{\gamma \in \{+, -\}} \gamma \hat{H}_{SB\gamma}(t')} \rho_{\text{tot}}(0) \right\} = \quad (26)$$

$$= \hat{\mathcal{V}}_0(t)\text{tr}_B \left\{ T_C \sum_{k=0}^{\infty} \frac{(-i)^k}{k!} \left[\int_0^t dt' \sum_{\gamma \in \{+, -\}} \gamma \hat{H}_{SB\gamma}(t') \right]^k \rho_{\text{tot}}(0) \right\} \quad (27)$$

We assume that there are initially no correlations between the system and the bath, that is $\rho_{\text{tot}}(0) = \rho(0) \otimes \rho_B$, such that we can perform the partial trace over bath operators stemming from $H_{SB}(t') = X(t') \otimes B(t')$, raised to the k -th power. We take the bath state to be stationary under the bare bath Hamiltonian, for example to be in equilibrium at some bath temperature, and, without loss of generality, we assume that $\text{tr}_B(B(t)\rho_B(0)) = \text{tr}_B(B\rho_B(0)) = 0$: a finite value of $\text{tr}_B(B\rho_B(0))$ could be in fact always absorbed in the definition of the Hamiltonian [30]. Under this assumption, only terms with even powers of k are non-zero, and therefore we change the summation index to sum only on those even terms. Finally we consider system and bath operators that are non-fermionic, such that they commute under time-ordering. Under these assumptions, we obtain

$$\begin{aligned} \hat{\mathcal{V}}(t)\rho(0) &= \hat{\mathcal{V}}_0(t) \sum_{k=0}^{\infty} \frac{(-i)^{2k}}{(2k)!} \int_0^t dt_1 \cdots \int_0^t dt_{2k} \times \\ &\sum_{\gamma_1 \cdots \gamma_{2k}} \gamma_1 \cdots \gamma_{2k} \text{tr}_B [T_C \hat{B}_{\gamma_1}(t_1) \cdots \hat{B}_{\gamma_{2k}}(t_{2k}) \rho_B(0)] T_C \hat{X}_{\gamma_1}(t_1) \cdots \hat{X}_{\gamma_{2k}}(t_{2k}) \rho(0) \end{aligned} \quad (28)$$

Since the bath Hamiltonian $H_B = \sum_i \omega_i a_i^\dagger a_i$ is quadratic in its creation and annihilation operators and assuming also its initial state $\rho_B(0)$ is, we can use the Wick's theorem to simplify the multi-point correlators of bath operators. For Hermitian bosonic operators such as $B = \sum_i \frac{\lambda_i}{2} (a_i + a_i^\dagger)$ one can use the Wick's theorem for real bosonic variables yielding

$$\text{tr}_B [T_C \hat{B}_{\gamma_1}(t_1) \cdots \hat{B}_{\gamma_{2k}}(t_{2k}) \rho_B(0)] = \sum_{\substack{\text{pairings of} \\ \{(t_1, t_1) \cdots (t_{2k}, t_{2k})\}}} \Gamma_{\gamma_{i_1} \gamma_{i_2}}(t_{i_1} - t_{i_2}) \cdots \Gamma_{\gamma_{i_{2k-1}} \gamma_{i_{2k}}}(t_{i_{2k-1}} - t_{i_{2k}}) \quad (29)$$

On the left-hand side, the two-point correlation functions of the bath appear

$$\Gamma_{\gamma,\gamma'}(t-t') = \text{tr}_B [T_C \hat{B}_\gamma(t) \hat{B}_{\gamma'}(t') \rho_B(0)], \quad (30)$$

which depend on time differences because we assumed $\rho_B(0)$ to be stationary, and the sum runs over all the possible ways of forming pairs with the indexes $\{(\gamma_1, t_1), \dots, (\gamma_{2k}, t_{2k})\}$. Also, since the integrand is completely symmetric by permuting two integration/summation indexes (t_i, γ_i) and (t_j, γ_j) , we can limit the integration to the domain defined by $t_1 > t_2 > \dots > t_{2k}$ and multiply by $(2k)!$. We can also drop the contour time-ordering operator T_C , which is at this point useless since time-ordering is already enforced by the extremes of integration. Finally, we write the string of system operators by making explicit their time-evolution as follows

$$\hat{\mathcal{V}}_0(t) \hat{X}_{\gamma_1}(t_1) \dots \hat{X}_{\gamma_{2k}}(t_{2k}) = \hat{\mathcal{V}}_0(t-t_1) \hat{X}_{\gamma_1} \hat{\mathcal{V}}_0(t_1-t_2) \dots \hat{X}_{\gamma_{2k}} \hat{\mathcal{V}}_0(t_{2k}) \quad (31)$$

and we drop the initial state $\rho(0)$, since this is arbitrary. Eventually, we obtain the series for the evolution superoperator $\hat{\mathcal{V}}$:

$$\hat{\mathcal{V}}(t) = \sum_{k=0}^{\infty} (-i)^{2k} \int_0^t dt_1 \int_0^{t_1} dt_2 \dots \int_0^{t_{2k-1}} dt_{2k} \sum_{\gamma_1 \dots \gamma_{2k}} \sum_{\substack{\text{pairings of} \\ \{(\gamma_1, t_1), \dots, (\gamma_{2k}, t_{2k})\}}} \Gamma_{\gamma_{i_1} \gamma_{i_2}}(t_{i_1} - t_{i_2}) \dots \Gamma_{\gamma_{i_{2k-1}} \gamma_{i_{2k}}}(t_{i_{2k-1}} - t_{i_{2k}}) \hat{\mathcal{V}}_0(t-t_1) \hat{X}_{\gamma_1} \hat{\mathcal{V}}_0(t_1-t_2) \hat{X}_{\gamma_2} \dots \hat{X}_{\gamma_{2k}} \hat{\mathcal{V}}_0(t_{2k}), \quad (32)$$

While it is possible to manipulate this series directly, it is more convenient for our purposes to show that it takes the form of the Dyson equation (4) of the main text and to introduce its self-energy. This is the object of the next section.

E.2 Feynman diagrams, self-energy and Dyson equation

In order to show that Eq. (32) can be cast in the Dyson form of Eq. (4) of the main text, we start by introducing its diagrammatic representation. Each term of the series with fixed $k, t_1 \dots t_{2k}, \gamma_1 \dots \gamma_{2k}$ and with a fixed choice of pairings can be represented as a Feynman diagram following these rules:

- draw two parallel solid lines, each representing a portion of time axis going from time $t = 0$ to time t .
- locate the $t_1 > \dots > t_{2k}$ times on those axes, where the k_+ times corresponding to an \hat{X}_+ superoperator must be drawn on the first time axis and the $k_- = k - k_+$ times corresponding to an \hat{X}_- superoperator on the other one. The couple of solid-line segments going from t_i to t_{i+1} represent the evolution superoperator $\hat{\mathcal{V}}_0(t_{i+1} - t_i)$.
- connect the times paired by Γ functions with dashed lines.

Finally, one also needs to keep track of the factor $(-1)^{2k}$ as well as of the sign given by the product $\gamma_1 \dots \gamma_{2k}$. As an example, the term with expression

$$\Gamma_{+-}(t_1 - t_2) \hat{\mathcal{V}}_0(t-t_1) \hat{X}_+ \hat{\mathcal{V}}_0(t_1-t_2) \hat{X}_- \hat{\mathcal{V}}_0(t_2) \bullet \quad (33)$$

corresponds to the diagram in Fig. 4:

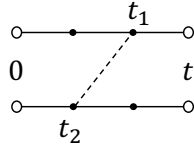


Figure 4: The diagrammatic representation of the term (33).

Summing over the γ indexes, one can also define more compact diagrams where the double-time axis is collapsed on a single time-axis, as shown in Fig. 5:

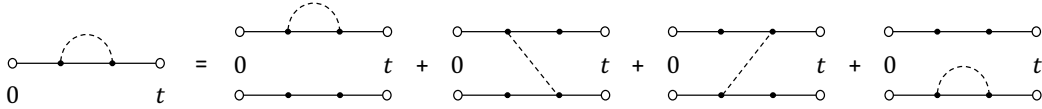


Figure 5: Single time-axis diagrams represent the set of diagrams where super-operator indexes are summed over.

From these diagrammatic rules, we can define a “self-energy” of the series on the lines of textbook calculations in many-body theory. For this purpose, we define as one-particle-irreducible (1PI) the compact diagrams which cannot be separated, by cutting a solid line, in two parts that are not connected by any dashed line. An example of 1PI diagrams is given in Fig. 6. Then, the self-energy \hat{D} is defined as the sum of all 1PI diagrams with the first and last solid lines removed: its diagrammatic representation is given in Fig. 6.

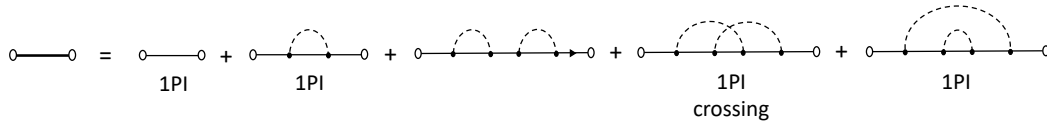


Figure 6: 1-particle-irreducible (1PI) diagrams making up the self-energy and crossing diagrams.

The superoperator $\hat{\mathcal{V}}$ is given by the sum of all diagrams, both 1PI and non-1PI. The definition of the self-energy is useful because all non-1PI diagrams can be obtained by joining some 1PI diagrams with solid lines and, therefore, the whole series for $\hat{\mathcal{V}}$ can be written as

$$\hat{\mathcal{V}} = \hat{\mathcal{V}}_0 + \hat{\mathcal{V}}_0 \circ \hat{D} \circ \hat{\mathcal{V}}_0 + \hat{\mathcal{V}}_0 \circ \hat{D} \circ \hat{\mathcal{V}}_0 \circ \hat{D} \circ \hat{\mathcal{V}}_0 + \dots,$$

where the circle operator “ \circ ” stands for partial time convolutions as in Eq. (32). This series sums up to the Dyson equation

$$\begin{aligned} \hat{\mathcal{V}}(t) &= \hat{\mathcal{V}}_0(t) + \int_0^t dt_1 \int_0^{t_1} dt_2 \hat{\mathcal{V}}_0(t-t_1) \hat{D}(t_1-t_2) \hat{\mathcal{V}}(t_2) \\ &= \hat{\mathcal{V}}_0(t) + \int_0^t dt_1 \int_0^{t_1} dt_2 \hat{\mathcal{V}}(t-t_1) \hat{D}(t_1-t_2) \hat{\mathcal{V}}_0(t_2) \end{aligned} \quad (34)$$

or equivalently, to the integro-differential form reported as Eq. (4) in the main text:

$$\partial_t \hat{\mathcal{V}}(t) = \hat{H}_S \hat{\mathcal{V}}(t) + \int_0^t dt_1 \hat{D}(t-t_1) \hat{\mathcal{V}}(t_1) \quad (35)$$

E.3 The non-crossing approximation

The non-crossing approximation (NCA) corresponds to approximating the series for $\hat{\mathcal{V}}$, and thus also for $\hat{\mathcal{D}}$, by keeping only the compact diagrams in which dashed lines do not cross. We remark that considering the compact diagrams is important for defining non-crossing diagrams, as in their non-compact version ambiguities arise as dashed lines might cross or not depending on how one draws them. An example of crossing diagram is given in Fig. 6 and the diagrammatic representation of the NCA self-energy is shown in Fig. 1.

It turns out that the NCA self-energy coincides with the $k = 1$ term of the exact self-energy, where the bare propagator $\hat{\mathcal{V}}_0$ is replaced with the dressed one $\hat{\mathcal{V}}$. This statement corresponds to the second equality in Fig. 1. In fact, we remark that the first and last times of a self-energy diagram must be connected together by a dashed line in the non-crossing approximation: if it's not the case, in fact, the resulting diagram is either non-1PI or it's crossed. We also remark that all diagrams with first and last time connected are necessarily 1PI. Therefore all the diagrams of $\hat{\mathcal{D}}_{\text{NCA}}$ are obtained connecting the remaining times in all possible non-crossing ways, but the latter diagrams in turn sum up to $\hat{\mathcal{V}}$, proving the equality.

The explicit expression of the NCA self-energy is then given by

$$\hat{\mathcal{D}}_{\text{NCA}}(\tau) = (-i)^2 \sum_{\gamma_1 \gamma_2} \gamma_1 \gamma_2 \Gamma_{\gamma_1 \gamma_2}(\tau) \hat{\mathcal{X}}_{\gamma_1} \hat{\mathcal{V}}(\tau) \hat{\mathcal{X}}_{\gamma_2}. \quad (36)$$

Carrying out the sum over γ indexes and after some algebraic manipulations to go from the time-ordered correlation function $\Gamma_{\gamma_1, \gamma_2}(\tau)$, defined in Eq. (30), to the non-time ordered correlation function $\Gamma(\tau)$, defined in Eq. (3) of the main text, the NCA self-energy reduces to Eq. (5) of the main text.

E.4 Validity of the NCA and Markov approximations together

We discuss in this appendix the validity of the NCA-Markov approximation, leading to Eq. (6) of the main text. At first glance the assumptions behind the NCA and Markovian approximations seem to contradict each other. The Markovian approximation assumes that the bath-induced dynamics on the timescale of bath correlation functions, call it τ_b , is negligible, thus one can approximate $\hat{\mathcal{V}}(t)$ with $e^{\hat{\mathcal{H}}_s \tau} \hat{\mathcal{V}}(t - \tau)$. The NCA self-energy, on the other hand, captures bath-induced processes happening on timescales shorter than τ_b . This contradiction is resolved and the two approximations can be made simultaneously, if one assumes that bath-induced dynamics, on a timescale τ_b , can be neglected only when $t > \tau_b$. In this way the Markovian approximation on the NCA master-equation is legitimate:

$$\begin{aligned} \partial_t \hat{\mathcal{V}}(t) &= \hat{\mathcal{H}}_S \hat{\mathcal{V}}(t) + \int_0^t d\tau [\Gamma(\tau)(-X_+ + X_-) \hat{\mathcal{V}}(\tau) X_+ + \text{H.c.}] \hat{\mathcal{V}}(t - \tau) \\ &\approx \hat{\mathcal{H}}_S \hat{\mathcal{V}}(t) + \int_0^t d\tau [\Gamma(\tau)(-X_+ + X_-) \hat{\mathcal{V}}(\tau) X_+ + \text{H.c.}] e^{-\hat{\mathcal{H}}_s \tau} \hat{\mathcal{V}}(t) \end{aligned} \quad (37)$$

where $\hat{\mathcal{V}}(t) \approx e^{\hat{\mathcal{H}}_s \tau} \hat{\mathcal{V}}(t - \tau)$ for $t > \tau_b$ has been approximate in the spirit of a Markovian approximation, while $\hat{\mathcal{V}}(\tau)$ is probed inside the integral only at times $\tau < \tau_b$ and thus bath-induced dynamics is not neglected for this propagator. The essence of the NCA-Markov approximation, therefore, is that the bath-induced dynamics at short times $t < \tau_b$ is feedbacked into the dynamics at $t > \tau_b$. To be fully consistent, one should evolve $\hat{\mathcal{V}}(t)$ up to $t \sim \tau_b$ with the non-Markovian

NCA equations and then continue the propagation using the NCA-Markov master equation. The results of the main text have been obtained instead by integrating the NCA-Markov equations from $t = 0$.

We remark that the dynamics on the timescale τ_b is left completely unresolved in most Markovian master equations [33, 101, 103], where the upper integration integral in Eq. (37) is sent to infinity.

E.5 Beyond NCA

It is possible to go systematically beyond the NCA, which is particularly useful to assess the validity of its predictions. The exact self-energy \hat{D} , which is represented in Fig. 1 as a series of diagrams in terms of the “bare” propagator $\hat{V}_0 = e^{\mathcal{H}_s \tau}$, can be also expressed as a series of “skeleton” (dressed) diagrams, which depend only on \hat{V} rather than on \hat{V}_0 . This is a standard result of many-body theory (see e.g. [99]). This skeleton series is defined by all the diagrams which have no self-energy insertions, that is no pieces that disconnect from the diagram by cutting two solid lines [99]. The NCA yields the first term of the skeleton series for the self-energy. We remark that each diagram of the skeleton series contains contributions up to all powers in the system-bath coupling. Nevertheless an “order” in the series exists such that higher-order diagrams are smaller than lower-order ones for a sufficiently weak coupling, as it is the case for the bare series. The natural strategy to assess the validity of the NCA results is therefore to include higher-order contributions to the self-energy. At sufficiently small coupling the NCA predictions become quantitatively accurate, as higher-order diagrams are negligible, while at stronger coupling one can still check qualitative agreement upon including higher-order terms. Adding the leading-order diagram beyond NCA yields the self-energy

$$\hat{D}_{\text{OCA}}(\tau) = \hat{D}_{\text{NCA}}(\tau) + (-i)^4 \sum_{\gamma_1 \gamma_2 \gamma_0 \gamma} \gamma_1 \gamma_2 \gamma_0 \gamma \times \int_0^\tau d\tau_1 \int_0^{\tau_1} d\tau_2 \Gamma_{\gamma\gamma_2}(\tau - \tau_2) \Gamma_{\gamma_1 \gamma_0}(\tau_1) \hat{X}_\gamma \hat{V}(\tau - \tau_1) \hat{X}_{\gamma_1} \hat{V}(\tau_1 - \tau_2) \hat{X}_{\gamma_2} \hat{V}(\tau_2) \hat{X}_{\gamma_0} \quad (38)$$

This is known as one-crossing approximation (OCA) [91, 100], as it corresponds to summing the bare diagrams in which 2 dashed lines, corresponding to bath 2-times correlation functions, cross at most once. The second term of (38) becomes smaller than the first at a small enough coupling, because it involves two bath correlation functions. As we mentioned in the main text, diagrams of the skeleton series are also ordered in terms of increasing decay-time of the self-energy or “memory” of the bath. In Fig. 1 we show that the NCA self-energy decays in a timescale $\tau \sim \tau_b$, in which the bath correlation function $\Gamma(\tau)$ decays: this is the case because $\hat{D}_{\text{NCA}}(\tau)$ is proportional to $\Gamma(\tau)$ (Eq. (5) of the main text). The second term in Eq. (38) instead decays in $2\tau_b$, because of the two bath correlation functions ($\Gamma_{\gamma\gamma'}$ reduces to Γ or to its complex conjugate given the time-ordering of its arguments).

An application of the OCA to the Spin-Boson model is reported in 3.2

F The Born-Markov master equation

A Markovian approximation of the Born master equation (1) leads to

$$\partial_t \rho(t) = \hat{\mathcal{H}}_S \rho(t) + \int_0^t d\tau \hat{\mathcal{D}}_{\text{Born}}(\tau) e^{-\hat{\mathcal{H}}_S \tau} \rho(t) \quad (39)$$

which together with (2) is the Born-Markov master equation, used in the main text for comparison with the NCA-Markov map.

The most common way of writing this equation (see e.g. [31]) is by explicitly replacing the self-energy (2) in (39) getting

$$\partial_t \rho(t) = -i[H_S, \rho(t)] + [X\tilde{X}\rho(t) + \tilde{X}\rho(t)X + \text{H.c.}] \quad (40)$$

in terms of the “filtered” operators

$$\tilde{X} = \int_0^t d\tau \Gamma(\tau) e^{-iH_S \tau} X e^{iH_S \tau} \quad (41)$$

In the main text, we always keep the integration time in (41) finite to compare with the NCA-Markov map.

Instead, when doing a Markovian approximation usually the integration in (41) is extended up to infinity [103], as bath correlation functions decay on a timescale $\tau \sim \tau_b$, while the system is assumed to change on a much slower timescale. This allows to evaluate the operator \tilde{X} in the basis of the eigenstates of the system $|E_n\rangle$ with eigenvalues E_n , where it is expressed in terms of the Fourier transform of the retarded component of the bath correlation function $\Gamma^R(\omega) = \int_{-\infty}^{\infty} d\tau e^{i\omega\tau} \Gamma(\tau) \theta(\tau)$:

$$\tilde{X} = \sum_{nm} \Gamma^R(E_m - E_n) \langle n|X|m\rangle |n\rangle \langle m| \quad (42)$$

G Further results on the Spin-Boson model

G.1 Steady state correlation functions

In the main text, we have discussed the transient dynamics of the Ohmic spin-boson model, while here we focus on its correlation functions computed once the steady-state of the dynamics has been reached.

In Fig. 7 we show the Fourier transform of the steady-state correlation function $C_z(t) = \frac{1}{2} \lim_{t' \rightarrow \infty} \langle [\sigma_z(t+t'), \sigma_z(t')] \rangle$, which is a purely real function, computed from Eq. (18). At weak coupling with the bath, this correlation function shows a peak at Δ , corresponding to spin-flip transitions at the frequency of the bare spin. Increasing the coupling to the bath, the spin frequency gets renormalized to a smaller value Δ_r , which appears as a shift of the corresponding peak in $C_z(\omega)$. The upper panel of Fig. 7 shows that, increasing the system-bath coupling, both the NCA and NCA-Markov approaches predict a renormalized value of Δ_r , which approaches $\Delta_r = 0$ as the critical coupling α_c is reached. This is known to happen [110] for the Ohmic spin-boson model at zero temperature for $\Delta/\omega_c \ll 1$. We remark that instead the dependence of Δ_r from α as it approaches the critical value, which is also known analytically, is not correctly reproduced by the

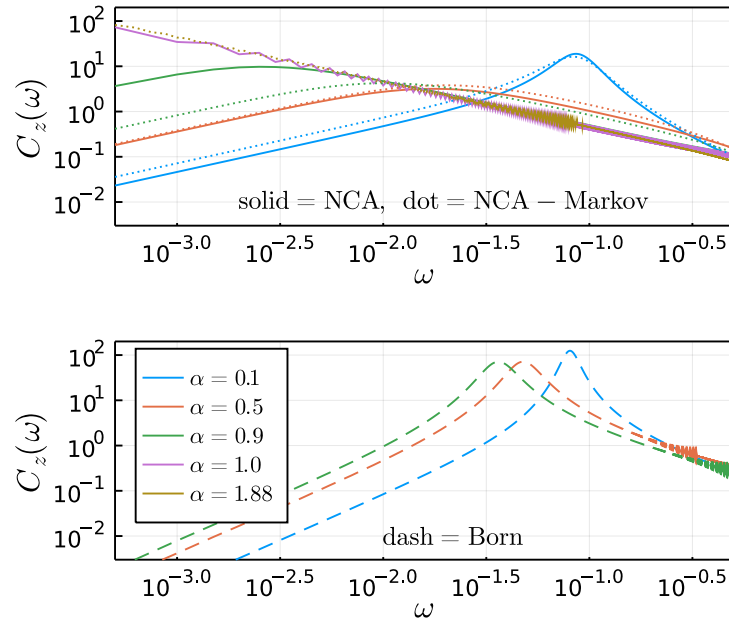


Figure 7: Steady-state correlation function of the z -spin component, $C_z(\omega)$ obtained through the NCA and NCA-Markov (top panel) quantum dynamical maps using Eq. (18), and their Born approximation (bottom panel). We see that both NCA approaches correctly capture the renormalization of the spin frequency Δ_r due to the bath coupling, ultimately leading to a quantum phase transition into a localized phase when $\Delta_r = 0$ for $\alpha = \alpha_c$. The low frequency behavior shows a power-law behavior of the form $C_z(\omega) \sim \omega$ as expected for an ohmic bath. On the other hand the Born approximation fails both in the capturing the frequency renormalization and in the power-law regime at low frequency, different from the expected linear behavior.

NCA approximation. The Born-Markov approximation is not shown in Fig. 7 as it is numerically unstable for $\alpha = 0.5, 0.9$ considered, while the Born approximation predicts only a very small shift of the peak, which never reaches zero for the values of coupling explored (up to $\alpha \approx 200$).

In addition, we also remark that the power-law behaviour of $C_z(\omega)$ at small ω is correctly captured in the NCA and NCA-Markov approximations, $C_z(\omega) \sim \omega$, while the Born approximation predicts $C_z(\omega) \sim \omega^2$.

G.2 Connections to experiments

In a recent experiment [48], the spin-boson model is realized by a superconducting transmission line, whose electromagnetic modes represent the bosonic environment, coupled to a qubit, realizing the two-state system. The response of the system can be probed by applying a weak probe field at a frequency ω to the transmission line and measuring its transmission

$$\mathcal{T}(\omega) = 1 - i\mathcal{N}\omega\chi(\omega) \quad (43)$$

where $\chi(\omega)(t - t') = -i\langle[\sigma^z(t), \sigma^z(t')]\rangle\theta(t)$ is the retarded Green function of σ^z and \mathcal{N} is a coupling constant that we set to $\mathcal{N} = 1$, as we aim at a qualitative comparison with Ref. [48].

The crossover between underdamped-coherent and incoherent dynamics of the spin boson model can be probed by transmission measurements scanning both the frequency of the probe ω and a static magnetic flux applied to the qubit ϵ , resulting in the qubit Hamiltonian

$$H_{\text{qb}} = \frac{\Delta}{2}\sigma^x + \frac{\epsilon}{2}\sigma^z \quad (44)$$

In Fig. 8 the color code indicates the modulus squared transmission $|\mathcal{T}(\omega)|^2$ as a function of ω and ϵ (in units of ω_c). The first column refers to the regime of underdamped-coherent dynamics for $\alpha = 0.1$ while the second column to the incoherent dynamics regime for $\alpha = 0.6$; the top panels are obtained using the NCA map, while the bottom ones with a Born master equation. The NCA results are in qualitative agreement with the experimental results of [48] (their Fig. 2), showing that the qubit dispersion relation can be read out of the transmission measurement in the underdamped-coherent regime (left panel), while in the incoherent regime (right panel) the transmission is nearly independent of the probe frequency ω . In the bottom panels we show that the Born master equation does not capture the transition to a regime of incoherent dynamics and always predicts a trace of the qubit dispersion in the transmission (bottom right panel). This result agrees with the results on the real-time dynamics described in the main text (Fig. 2). We also remark that the Born master equation wrongly predicts enhanced, rather than suppressed, transmission for values of ω and ϵ hitting the qubit dispersion for $\alpha = 0.1$ (left plot).

G.3 Steady-state dependence in NCA vs Born

The steady-state equation (17) also allows to understand why the NCA approaches capture the dependence of the steady-state on the system-bath coupling α in the top panels of Fig. 2 of the main text, which is instead missing in Born and Born-Markov theories: from our calculations we find that the steady-state of the spin-boson model does not depend on the Hamiltonian and takes the form $\rho_s = p_-|-\rangle\langle-| + p_+|+\rangle\langle+|$. In this case then Eq. (17) reduces to $\int_0^\infty d\tau \hat{D}(\tau)\rho_s = 0$.

By expanding the self-energy $\hat{D}(\tau)$ in powers of the system-bath coupling α as $\hat{D}(\tau) = \alpha\hat{D}^{(1)}(\tau) + \alpha^2\hat{D}^{(2)}(\tau) + \dots$, the Born and Born-Markov approximations correspond to truncating at first order in α and thus α drops in the steady-state equation: $\int_0^\infty d\tau \hat{D}^{(1)}(\tau)\rho_s = 0$.

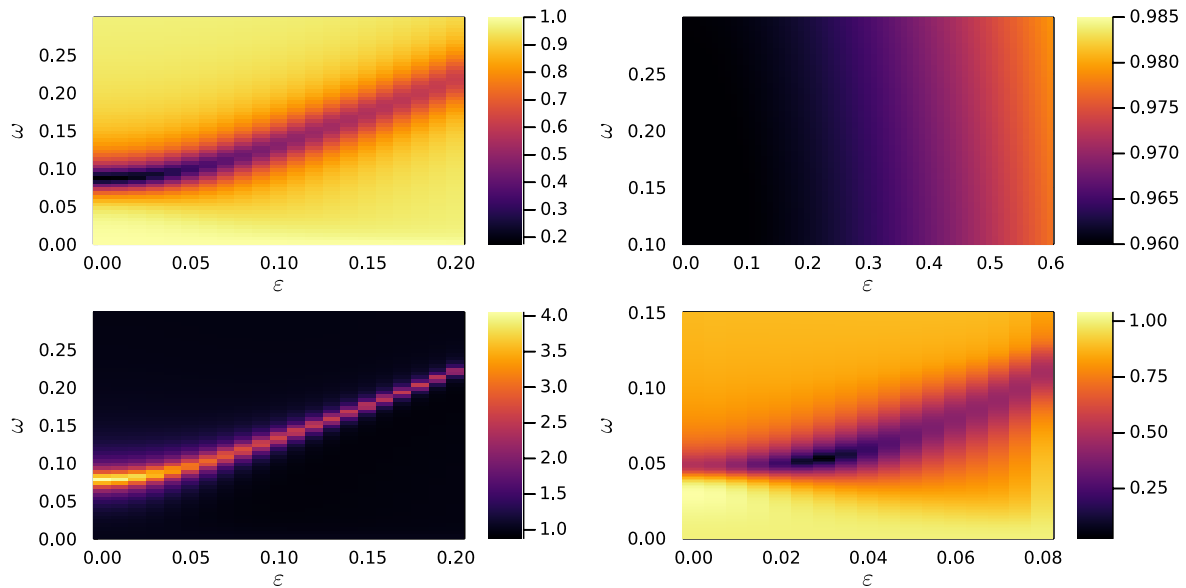


Figure 8: Modulus squared transmission $|\mathcal{T}(\omega)|^2$ of an applied probe field of frequency ω as a function of the two-level system bias ϵ . The top panels are obtained using the NCA map, while the bottom ones with a Born master equation. Left(right) panels correspond to the regime of underdamped-coherent (incoherent) dynamics for $\alpha = 0.1(0.6)$. The NCA map captures the crossover between underdamped and incoherent dynamics, while the Born master equation always predict an underdamped dynamics.

Instead, the NCA and NCA-Markov approaches retain higher-order contributions to the self-energy, yielding a non-trivial dependence of the steady-state on α .

References

- [1] R. K. Wangsness and F. Bloch, The Dynamical Theory of Nuclear Induction, Phys. Rev. **89**(4), 728 (1953), doi:[10.1103/PhysRev.89.728](https://doi.org/10.1103/PhysRev.89.728).
- [2] A. G. Redfield, On the Theory of Relaxation Processes, IBM Journal of Research and Development **1**(1), 19 (1957), doi:[10.1147/rd.11.0019](https://doi.org/10.1147/rd.11.0019).
- [3] R. Kubo, A Stochastic Theory of Line Shape, In *Advances in Chemical Physics*, pp. 101–127. John Wiley & Sons, Ltd, ISBN 978-0-470-14360-5, doi:[10.1002/9780470143605.ch6](https://doi.org/10.1002/9780470143605.ch6) (1969).
- [4] M. O. Scully and W. E. Lamb, Quantum Theory of an Optical Maser. I. General Theory, Phys. Rev. **159**(2), 208 (1967), doi:[10.1103/PhysRev.159.208](https://doi.org/10.1103/PhysRev.159.208).
- [5] B. R. Mollow and M. M. Miller, The damped driven two-level atom, Annals of Physics **52**(3), 464 (1969), doi:[10.1016/0003-4916\(69\)90289-9](https://doi.org/10.1016/0003-4916(69)90289-9).

- [6] G. McCauley, B. Cruikshank, S. Santra and K. Jacobs, Ability of Markovian master equations to model quantum computers and other systems under broadband control, Phys. Rev. Research **2**(1), 013049 (2020), doi:[10.1103/PhysRevResearch.2.013049](https://doi.org/10.1103/PhysRevResearch.2.013049).
- [7] Z. Leghtas, S. Touzard, I. M. Pop, A. Kou, B. Vlastakis, A. Petrenko, K. M. Sliwa, A. Narla, S. Shankar, M. J. Hatridge, M. Reagor, L. Frunzio et al., Confining the state of light to a quantum manifold by engineered two-photon loss, Science **347**(6224), 853 (2015), doi:[10.1126/science.aaa2085](https://doi.org/10.1126/science.aaa2085).
- [8] V. Giovannetti, S. Lloyd and L. Maccone, Advances in quantum metrology, Nature Photon **5**(4), 222 (2011), doi:[10.1038/nphoton.2011.35](https://doi.org/10.1038/nphoton.2011.35).
- [9] S. Vinjanampathy and J. Anders, Quantum thermodynamics, Contemporary Physics **57**(4), 545 (2016), doi:[10.1080/00107514.2016.1201896](https://doi.org/10.1080/00107514.2016.1201896).
- [10] P. Kómár, E. M. Kessler, M. Bishof, L. Jiang, A. S. Sørensen, J. Ye and M. D. Lukin, A quantum network of clocks, Nature Phys **10**(8), 582 (2014), doi:[10.1038/nphys3000](https://doi.org/10.1038/nphys3000).
- [11] P. Gehring, J. M. Thijssen and H. S. J. van der Zant, Single-molecule quantum-transport phenomena in break junctions, Nat Rev Phys **1**(6), 381 (2019), doi:[10.1038/s42254-019-0055-1](https://doi.org/10.1038/s42254-019-0055-1).
- [12] P. Hänggi, P. Talkner and M. Borkovec, Reaction-rate theory: Fifty years after Kramers, Rev. Mod. Phys. **62**(2), 251 (1990), doi:[10.1103/RevModPhys.62.251](https://doi.org/10.1103/RevModPhys.62.251).
- [13] P. G. Wolynes, Quantum Theory of Activated Events in Condensed Phases, Phys. Rev. Lett. **47**(13), 968 (1981), doi:[10.1103/PhysRevLett.47.968](https://doi.org/10.1103/PhysRevLett.47.968).
- [14] G. A. Voth, D. Chandler and W. H. Miller, Rigorous formulation of quantum transition state theory and its dynamical corrections, J. Chem. Phys. **91**(12), 7749 (1989), doi:[10.1063/1.457242](https://doi.org/10.1063/1.457242).
- [15] R. Ianculescu and E. Pollak, Activated quantum diffusion in a periodic potential above the crossover temperature, J. Chem. Phys. **151**(2), 024703 (2019), doi:[10.1063/1.5100010](https://doi.org/10.1063/1.5100010).
- [16] G. S. Engel, T. R. Calhoun, E. L. Read, T.-K. Ahn, T. Mančal, Y.-C. Cheng, R. E. Blankenship and G. R. Fleming, Evidence for wavelike energy transfer through quantum coherence in photosynthetic systems, Nature **446**(7137), 782 (2007), doi:[10.1038/nature05678](https://doi.org/10.1038/nature05678).
- [17] G. Panitchayangkoon, D. Hayes, K. A. Fransted, J. R. Caram, E. Harel, J. Wen, R. E. Blankenship and G. S. Engel, Long-lived quantum coherence in photosynthetic complexes at physiological temperature, PNAS **107**(29), 12766 (2010).
- [18] E. Collini, C. Y. Wong, K. E. Wilk, P. M. G. Curmi, P. Brumer and G. D. Scholes, Coherently wired light-harvesting in photosynthetic marine algae at ambient temperature, Nature **463**(7281), 644 (2010), doi:[10.1038/nature08811](https://doi.org/10.1038/nature08811).
- [19] R. E. Blankenship, D. M. Tiede, J. Barber, G. W. Brudvig, G. Fleming, M. Ghirardi, M. R. Gunner, W. Junge, D. M. Kramer, A. Melis, T. A. Moore, C. C. Moser et al., Comparing Photosynthetic and Photovoltaic Efficiencies and Recognizing the Potential for Improvement, Science **332**(6031), 805 (2011), doi:[10.1126/science.1200165](https://doi.org/10.1126/science.1200165).

- [20] N. Lambert, Y.-N. Chen, Y.-C. Cheng, C.-M. Li, G.-Y. Chen and F. Nori, Quantum biology, *Nature Phys* **9**(1), 10 (2013), doi:[10.1038/nphys2474](https://doi.org/10.1038/nphys2474).
- [21] J. Cao, R. J. Cogdell, D. F. Coker, H.-G. Duan, J. Hauer, U. Kleinekathöfer, T. L. C. Jansen, T. Mančal, R. J. D. Miller, J. P. Ogilvie, V. I. Prokhorenko, T. Renger et al., Quantum biology revisited, *Sci. Adv.* **6**(14), eaaz4888 (2020), doi:[10.1126/sciadv.aaz4888](https://doi.org/10.1126/sciadv.aaz4888).
- [22] E. Kapit, M. Hafezi and S. H. Simon, Induced Self-Stabilization in Fractional Quantum Hall States of Light, *Phys. Rev. X* **4**(3), 031039 (2014), doi:[10.1103/PhysRevX.4.031039](https://doi.org/10.1103/PhysRevX.4.031039).
- [23] R. Ma, B. Saxberg, C. Owens, N. Leung, Y. Lu, J. Simon and D. I. Schuster, A dissipatively stabilized Mott insulator of photons, *Nature* **566**(7742), 51 (2019), doi:[10.1038/s41586-019-0897-9](https://doi.org/10.1038/s41586-019-0897-9).
- [24] J. Puertas Martínez, S. Léger, N. Gheeraert, R. Dassonneville, L. Planat, F. Foroughi, Y. Krupko, O. Buisson, C. Naud, W. Hasch-Guichard, S. Florens, I. Snyman et al., A tunable Josephson platform to explore many-body quantum optics in circuit-QED, *npj Quantum Inf* **5**(1), 19 (2019), doi:[10.1038/s41534-018-0104-0](https://doi.org/10.1038/s41534-018-0104-0).
- [25] I. Carusotto, A. A. Houck, A. J. Kollár, P. Roushan, D. I. Schuster and J. Simon, Photonic materials in circuit quantum electrodynamics, *Nat. Phys.* **16**(3), 268 (2020), doi:[10.1038/s41567-020-0815-y](https://doi.org/10.1038/s41567-020-0815-y).
- [26] M. O. Scully and M. S. Zubairy, Quantum Optics, Cambridge University Press, Cambridge, ISBN 978-0-511-81399-3 (1997).
- [27] E. B. Davies, Markovian master equations, *Commun.Math. Phys.* **39**(2), 91 (1974), doi:[10.1007/BF01608389](https://doi.org/10.1007/BF01608389).
- [28] G. Lindblad, On the generators of quantum dynamical semigroups, *Communications in Mathematical Physics* **48**(2), 119 (1976), doi:[10.1007/BF01608499](https://doi.org/10.1007/BF01608499).
- [29] R. Dümcke and H. Spohn, The proper form of the generator in the weak coupling limit, *Z Physik B* **34**(4), 419 (1979), doi:[10.1007/BF01325208](https://doi.org/10.1007/BF01325208).
- [30] F. Nathan and M. S. Rudner, Universal Lindblad equation for open quantum systems, *Phys. Rev. B* **102**(11), 115109 (2020), doi:[10.1103/PhysRevB.102.115109](https://doi.org/10.1103/PhysRevB.102.115109).
- [31] E. Mozgunov and D. Lidar, Completely positive master equation for arbitrary driving and small level spacing, *Quantum* **4**, 227 (2020), doi:[10.22331/q-2020-02-06-227](https://doi.org/10.22331/q-2020-02-06-227).
- [32] G. McCauley, B. Cruikshank, D. I. Bondar and K. Jacobs, Accurate Lindblad-form master equation for weakly damped quantum systems across all regimes, *npj Quantum Inf* **6**(1), 1 (2020), doi:[10.1038/s41534-020-00299-6](https://doi.org/10.1038/s41534-020-00299-6).
- [33] D. Davidović, Completely Positive, Simple, and Possibly Highly Accurate Approximation of the Redfield Equation, *Quantum* **4**, 326 (2020), doi:[10.22331/q-2020-09-21-326](https://doi.org/10.22331/q-2020-09-21-326).
- [34] A. Trushechkin, Unified GKLS quantum master equation of weak-coupling limit type, arXiv:2103.12042 [math-ph, physics:quant-ph] (2021).

- [35] T. Becker, L.-N. Wu and A. Eckardt, Lindbladian approximation beyond ultra-weak coupling (2021), [2012.14208](https://arxiv.org/abs/2012.14208).
- [36] J. Dalibard, Y. Castin and K. Mølmer, Wave-function approach to dissipative processes in quantum optics, Phys. Rev. Lett. **68**(5), 580 (1992), doi:[10.1103/PhysRevLett.68.580](https://doi.org/10.1103/PhysRevLett.68.580).
- [37] R. Dum, P. Zoller and H. Ritsch, Monte Carlo simulation of the atomic master equation for spontaneous emission, Phys. Rev. A **45**(7), 4879 (1992), doi:[10.1103/PhysRevA.45.4879](https://doi.org/10.1103/PhysRevA.45.4879).
- [38] C. W. Gardiner and P. Zoller, Quantum Noise: A Handbook of Markovian and Non-Markovian Quantum Stochastic Methods with Applications to Quantum Optics, Springer Series in Synergetics. Springer, Berlin ; New York, 3rd ed edn., ISBN 978-3-540-22301-6 (2004).
- [39] M. Esposito and M. Galperin, Transport in molecular states language: Generalized quantum master equation approach, Phys. Rev. B **79**(20), 205303 (2009), doi:[10.1103/PhysRevB.79.205303](https://doi.org/10.1103/PhysRevB.79.205303).
- [40] M. Esposito and M. Galperin, Self-Consistent Quantum Master Equation Approach to Molecular Transport, J. Phys. Chem. C **114**(48), 20362 (2010), doi:[10.1021/jp103369s](https://doi.org/10.1021/jp103369s).
- [41] J. Jin, J. Li, Y. Liu, X.-Q. Li and Y. Yan, Improved master equation approach to quantum transport: From Born to self-consistent Born approximation, The Journal of Chemical Physics **140**(24), 244111 (2014), doi:[10.1063/1.4884390](https://doi.org/10.1063/1.4884390).
- [42] J. K. Sowa, J. A. Mol, G. A. D. Briggs and E. M. Gauger, Beyond Marcus theory and the Landauer-Büttiker approach in molecular junctions: A unified framework, The Journal of Chemical Physics **149**(15), 154112 (2018), doi:[10.1063/1.5049537](https://doi.org/10.1063/1.5049537).
- [43] J. K. Sowa, N. Lambert, T. Seideman and E. M. Gauger, Beyond Marcus theory and the Landauer-Büttiker approach in molecular junctions. II. A self-consistent Born approach, J. Chem. Phys. **152**(6), 064103 (2020), doi:[10.1063/1.5143146](https://doi.org/10.1063/1.5143146).
- [44] S. Gröblacher, A. Trubarov, N. Prigge, G. D. Cole, M. Aspelmeyer and J. Eisert, Observation of non-Markovian micromechanical Brownian motion, Nat Commun **6**(1), 7606 (2015), doi:[10.1038/ncomms8606](https://doi.org/10.1038/ncomms8606).
- [45] K. H. Madsen, S. Ates, T. Lund-Hansen, A. Löffler, S. Reitzenstein, A. Forchel and P. Lodahl, Observation of Non-Markovian Dynamics of a Single Quantum Dot in a Micropillar Cavity, Physical Review Letters **106**(23), 233601 (2011), doi:[10.1103/PhysRevLett.106.233601](https://doi.org/10.1103/PhysRevLett.106.233601).
- [46] X. Mi, J. V. Cady, D. M. Zajac, P. W. Deelman and J. R. Petta, Strong coupling of a single electron in silicon to a microwave photon, Science **355**(6321), 156 (2017), doi:[10.1126/science.aal2469](https://doi.org/10.1126/science.aal2469).
- [47] J. Puertas Martínez, S. Léger, N. Gheeraert, R. Dassonneville, L. Planat, F. Foroughi, Y. Krupko, O. Buisson, C. Naud, W. Hasch-Guichard, S. Florens, I. Snyman et al., A tunable Josephson platform to explore many-body quantum optics in circuit-QED, npj Quantum Inf **5**(1), 19 (2019), doi:[10.1038/s41534-018-0104-0](https://doi.org/10.1038/s41534-018-0104-0).

- [48] L. Magazzù, P. Forn-Díaz, R. Belyansky, J.-L. Orgiazzi, M. A. Yurtalan, M. R. Otto, A. Lupascu, C. M. Wilson and M. Grifoni, Probing the strongly driven spin-boson model in a superconducting quantum circuit, Nat Commun **9**(1), 1403 (2018), doi:[10.1038/s41467-018-03626-w](https://doi.org/10.1038/s41467-018-03626-w).
- [49] A. W. Chin, J. Prior, R. Rosenbach, F. Caycedo-Soler, S. F. Huelga and M. B. Plenio, The role of non-equilibrium vibrational structures in electronic coherence and recoherence in pigment–protein complexes, Nature Physics **9**(2), 113 (2013), doi:[10.1038/nphys2515](https://doi.org/10.1038/nphys2515).
- [50] R. Hanson, V. V. Dobrovitski, A. E. Feiguin, O. Gywat and D. D. Awschalom, Coherent Dynamics of a Single Spin Interacting with an Adjustable Spin Bath, Science **320**(5874), 352 (2008), doi:[10.1126/science.1155400](https://doi.org/10.1126/science.1155400).
- [51] M. Lebrat, P. Grišins, D. Husmann, S. Häusler, L. Corman, T. Giamarchi, J.-P. Brantut and T. Esslinger, Band and Correlated Insulators of Cold Fermions in a Mesoscopic Lattice, Phys. Rev. X **8**(1), 011053 (2018), doi:[10.1103/PhysRevX.8.011053](https://doi.org/10.1103/PhysRevX.8.011053).
- [52] B.-H. Liu, L. Li, Y.-F. Huang, C.-F. Li, G.-C. Guo, E.-M. Laine, H.-P. Breuer and J. Piilo, Experimental control of the transition from Markovian to non-Markovian dynamics of open quantum systems, Nature Phys **7**(12), 931 (2011), doi:[10.1038/nphys2085](https://doi.org/10.1038/nphys2085).
- [53] C. Maier, T. Brydges, P. Jurcevic, N. Trautmann, C. Hempel, B. P. Lanyon, P. Hauke, R. Blatt and C. F. Roos, Environment-Assisted Quantum Transport in a 10-qubit Network, Phys. Rev. Lett. **122**(5), 050501 (2019), doi:[10.1103/PhysRevLett.122.050501](https://doi.org/10.1103/PhysRevLett.122.050501).
- [54] A. Recati, P. O. Fedichev, W. Zwerger, J. von Delft and P. Zoller, Atomic Quantum Dots Coupled to a Reservoir of a Superfluid Bose-Einstein Condensate, Phys. Rev. Lett. **94**(4), 040404 (2005), doi:[10.1103/PhysRevLett.94.040404](https://doi.org/10.1103/PhysRevLett.94.040404).
- [55] I. de Vega and D. Alonso, Dynamics of non-markovian open quantum systems, Rev. Mod. Phys. **89**, 015001 (2017), doi:[10.1103/RevModPhys.89.015001](https://doi.org/10.1103/RevModPhys.89.015001).
- [56] C.-F. Li, G.-C. Guo and J. Piilo, Non-Markovian quantum dynamics: What is it good for?, EPL **128**(3), 30001 (2020), doi:[10.1209/0295-5075/128/30001](https://doi.org/10.1209/0295-5075/128/30001).
- [57] A. W. Chin, S. F. Huelga and M. B. Plenio, Quantum Metrology in Non-Markovian Environments, Phys. Rev. Lett. **109**(23), 233601 (2012), doi:[10.1103/PhysRevLett.109.233601](https://doi.org/10.1103/PhysRevLett.109.233601).
- [58] R. Alicki, M. Horodecki, P. Horodecki and R. Horodecki, Dynamical description of quantum computing: Generic nonlocality of quantum noise, Phys. Rev. A **65**(6), 062101 (2002), doi:[10.1103/PhysRevA.65.062101](https://doi.org/10.1103/PhysRevA.65.062101).
- [59] Y. Dong, Y. Zheng, S. Li, C.-C. Li, X.-D. Chen, G.-C. Guo and F.-W. Sun, Non-Markovianity-assisted high-fidelity Deutsch–Jozsa algorithm in diamond, npj Quantum Inf **4**(1), 1 (2018), doi:[10.1038/s41534-017-0053-z](https://doi.org/10.1038/s41534-017-0053-z).
- [60] A. Shabani and D. A. Lidar, Completely positive post-Markovian master equation via a measurement approach, Phys. Rev. A **71**(2), 020101 (2005), doi:[10.1103/PhysRevA.71.020101](https://doi.org/10.1103/PhysRevA.71.020101).

- [61] S. Maniscalco and F. Petruccione, Non-Markovian dynamics of a qubit, Phys. Rev. A **73**(1), 012111 (2006), doi:[10.1103/PhysRevA.73.012111](https://doi.org/10.1103/PhysRevA.73.012111).
- [62] D. Chruściński and A. Kossakowski, Non-Markovian Quantum Dynamics: Local versus Nonlocal, Phys. Rev. Lett. **104**(7), 070406 (2010), doi:[10.1103/PhysRevLett.104.070406](https://doi.org/10.1103/PhysRevLett.104.070406).
- [63] H. Schoeller and G. Schön, Mesoscopic quantum transport: Resonant tunneling in the presence of a strong Coulomb interaction, Phys. Rev. B **50**(24), 18436 (1994), doi:[10.1103/PhysRevB.50.18436](https://doi.org/10.1103/PhysRevB.50.18436).
- [64] H. Schoeller, A perturbative nonequilibrium renormalization group method for dissipative quantum mechanics: Real-time RG in frequency space (RTRG-FS), Eur. Phys. J. Spec. Top. **168**(1), 179 (2009), doi:[10.1140/epjst/e2009-00962-3](https://doi.org/10.1140/epjst/e2009-00962-3).
- [65] C. Karlewski and M. Marthaler, Time-local master equation connecting the Born and Markov approximations, Phys. Rev. B **90**(10), 104302 (2014), doi:[10.1103/PhysRevB.90.104302](https://doi.org/10.1103/PhysRevB.90.104302).
- [66] C. Müller and T. M. Stace, Deriving Lindblad master equations with Keldysh diagrams: Correlated gain and loss in higher order perturbation theory, Phys. Rev. A **95**(1), 013847 (2017), doi:[10.1103/PhysRevA.95.013847](https://doi.org/10.1103/PhysRevA.95.013847).
- [67] C. J. Lindner and H. Schoeller, Dissipative quantum mechanics beyond the Bloch-Redfield approximation: A consistent weak-coupling expansion of the Ohmic spin boson model at arbitrary bias, Phys. Rev. B **98**(11), 115425 (2018), doi:[10.1103/PhysRevB.98.115425](https://doi.org/10.1103/PhysRevB.98.115425).
- [68] E. Kleinherbers, N. Szpak, J. König and R. Schützhold, Relaxation dynamics in a Hubbard dimer coupled to fermionic baths: Phenomenological description and its microscopic foundation, Phys. Rev. B **101**(12), 125131 (2020), doi:[10.1103/PhysRevB.101.125131](https://doi.org/10.1103/PhysRevB.101.125131).
- [69] L. Mühlbacher and E. Rabani, Real-time path integral approach to nonequilibrium many-body quantum systems, Phys. Rev. Lett. **100**, 176403 (2008), doi:[10.1103/PhysRevLett.100.176403](https://doi.org/10.1103/PhysRevLett.100.176403).
- [70] M. Schiró and M. Fabrizio, Real-time diagrammatic monte carlo for nonequilibrium quantum transport, Phys. Rev. B **79**, 153302 (2009), doi:[10.1103/PhysRevB.79.153302](https://doi.org/10.1103/PhysRevB.79.153302).
- [71] P. Werner, T. Oka and A. J. Millis, Diagrammatic monte carlo simulation of nonequilibrium systems, Phys. Rev. B **79**, 035320 (2009), doi:[10.1103/PhysRevB.79.035320](https://doi.org/10.1103/PhysRevB.79.035320).
- [72] G. Cohen, E. Gull, D. R. Reichman and A. J. Millis, Green's functions from real-time bold-line monte carlo calculations: Spectral properties of the nonequilibrium anderson impurity model, Phys. Rev. Lett. **112**, 146802 (2014), doi:[10.1103/PhysRevLett.112.146802](https://doi.org/10.1103/PhysRevLett.112.146802).
- [73] G. Cohen, E. Gull, D. R. Reichman and A. J. Millis, Taming the dynamical sign problem in real-time evolution of quantum many-body problems, Phys. Rev. Lett. **115**, 266802 (2015), doi:[10.1103/PhysRevLett.115.266802](https://doi.org/10.1103/PhysRevLett.115.266802).
- [74] H.-T. Chen, G. Cohen and D. R. Reichman, Inchworm Monte Carlo for exact non-adiabatic dynamics. I. Theory and algorithms, J. Chem. Phys. **146**(5), 054105 (2017), doi:[10.1063/1.4974328](https://doi.org/10.1063/1.4974328).

- [75] H.-T. Chen, G. Cohen and D. R. Reichman, Inchworm Monte Carlo for exact non-adiabatic dynamics. II. Benchmarks and comparison with established methods, *J. Chem. Phys.* **146**(5), 054106 (2017), doi:[10.1063/1.4974329](https://doi.org/10.1063/1.4974329).
- [76] J. Jin, X. Zheng and Y. Yan, Exact dynamics of dissipative electronic systems and quantum transport: Hierarchical equations of motion approach, *The Journal of Chemical Physics* **128**(23), 234703 (2008), doi:[10.1063/1.2938087](https://doi.org/10.1063/1.2938087).
- [77] R. Härtle, G. Cohen, D. R. Reichman and A. J. Millis, Decoherence and lead-induced interdot coupling in nonequilibrium electron transport through interacting quantum dots: A hierarchical quantum master equation approach, *Phys. Rev. B* **88**(23), 235426 (2013), doi:[10.1103/PhysRevB.88.235426](https://doi.org/10.1103/PhysRevB.88.235426).
- [78] Y. Tanimura, Numerically “exact” approach to open quantum dynamics: The hierarchical equations of motion (HEOM), *J. Chem. Phys.* **153**(2), 020901 (2020), doi:[10.1063/5.0011599](https://doi.org/10.1063/5.0011599).
- [79] L. Diósi and W. T. Strunz, The non-Markovian stochastic Schrödinger equation for open systems, *Physics Letters A* **235**(6), 569 (1997), doi:[10.1016/S0375-9601\(97\)00717-2](https://doi.org/10.1016/S0375-9601(97)00717-2).
- [80] L. Diósi, N. Gisin and W. T. Strunz, Non-Markovian quantum state diffusion, *Phys. Rev. A* **58**(3), 1699 (1998), doi:[10.1103/PhysRevA.58.1699](https://doi.org/10.1103/PhysRevA.58.1699).
- [81] P. Gaspard and M. Nagaoka, Non-Markovian stochastic Schrödinger equation, *J. Chem. Phys.* **111**(13), 5676 (1999), doi:[10.1063/1.479868](https://doi.org/10.1063/1.479868).
- [82] J. Jing, X. Zhao, J. Q. You and T. Yu, Time-local quantum-state-diffusion equation for multilevel quantum systems, *Phys. Rev. A* **85**(4), 042106 (2012), doi:[10.1103/PhysRevA.85.042106](https://doi.org/10.1103/PhysRevA.85.042106).
- [83] D. Suess, A. Eisfeld and W. T. Strunz, Hierarchy of Stochastic Pure States for Open Quantum System Dynamics, *Phys. Rev. Lett.* **113**(15), 150403 (2014), doi:[10.1103/PhysRevLett.113.150403](https://doi.org/10.1103/PhysRevLett.113.150403).
- [84] J. Thoenniss, M. Sonner, A. Lerose and D. A. Abanin, An efficient method for quantum impurity problems out of equilibrium (2022).
- [85] A. Strathearn, P. Kirton, D. Kilda, J. Keeling and B. W. Lovett, Efficient non-Markovian quantum dynamics using time-evolving matrix product operators, *Nat Commun* **9**(1), 3322 (2018), doi:[10.1038/s41467-018-05617-3](https://doi.org/10.1038/s41467-018-05617-3).
- [86] H. Bruus and K. Flensberg, Many-Body Quantum Theory in Condensed Matter Physics : An Introduction, Oxford University Press, ISBN 978-0-19-856633-5 (2004).
- [87] A. Altland and B. D. Simons, Condensed Matter Field Theory, Cambridge University Press, 2 edn., doi:[10.1017/CBO9780511789984](https://doi.org/10.1017/CBO9780511789984) (2010).
- [88] N. E. Bickers, Review of techniques in the large- N expansion for dilute magnetic alloys, *Rev. Mod. Phys.* **59**(4), 845 (1987), doi:[10.1103/RevModPhys.59.845](https://doi.org/10.1103/RevModPhys.59.845).
- [89] E. Müller-Hartmann, Self-consistent perturbation theory of the anderson model: Ground state properties, *Z. Physik B - Condensed Matter* **57**(4), 281 (1984), doi:[10.1007/BF01470417](https://doi.org/10.1007/BF01470417).

- [90] P. Nordlander, M. Pustilnik, Y. Meir, N. S. Wingreen and D. C. Langreth, How long does it take for the kondo effect to develop?, Phys. Rev. Lett. **83**, 808 (1999), doi:[10.1103/PhysRevLett.83.808](https://doi.org/10.1103/PhysRevLett.83.808).
- [91] M. Eckstein and P. Werner, Nonequilibrium dynamical mean-field calculations based on the noncrossing approximation and its generalizations, Phys. Rev. B **82**(11), 115115 (2010), doi:[10.1103/PhysRevB.82.115115](https://doi.org/10.1103/PhysRevB.82.115115).
- [92] H.-T. Chen, G. Cohen, A. J. Millis and D. R. Reichman, Anderson-holstein model in two flavors of the noncrossing approximation, Phys. Rev. B **93**, 174309 (2016), doi:[10.1103/PhysRevB.93.174309](https://doi.org/10.1103/PhysRevB.93.174309).
- [93] Y. Meir, N. S. Wingreen and P. A. Lee, Low-temperature transport through a quantum dot: The anderson model out of equilibrium, Phys. Rev. Lett. **70**, 2601 (1993), doi:[10.1103/PhysRevLett.70.2601](https://doi.org/10.1103/PhysRevLett.70.2601).
- [94] T. Pruschke, D. L. Cox and M. Jarrell, Hubbard model at infinite dimensions: Thermodynamic and transport properties, Phys. Rev. B **47**(7), 3553 (1993), doi:[10.1103/PhysRevB.47.3553](https://doi.org/10.1103/PhysRevB.47.3553).
- [95] A. Erpenbeck, E. Gull and G. Cohen, Revealing strong correlations in higher-order transport statistics: A noncrossing approximation approach, Phys. Rev. B **103**, 125431 (2021), doi:[10.1103/PhysRevB.103.125431](https://doi.org/10.1103/PhysRevB.103.125431).
- [96] R. Härtle, G. Cohen, D. R. Reichman and A. J. Millis, Decoherence and lead-induced interdot coupling in nonequilibrium electron transport through interacting quantum dots: A hierarchical quantum master equation approach, Phys. Rev. B **88**, 235426 (2013), doi:[10.1103/PhysRevB.88.235426](https://doi.org/10.1103/PhysRevB.88.235426).
- [97] M. Schiró and O. Scarlatella, Quantum impurity models coupled to Markovian and non-Markovian baths, The Journal of Chemical Physics **151**(4), 044102 (2019), doi:[10.1063/1.5100157](https://doi.org/10.1063/1.5100157).
- [98] H. P. Breuer and F. Petruccione, The Theory of Open Quantum Systems, vol. 9780199213, OUP Oxford, 1st ed edn., ISBN 978-0-19-170634-9, doi:[10.1093/acprof:oso/9780199213900.001.0001](https://doi.org/10.1093/acprof:oso/9780199213900.001.0001) (2007).
- [99] G. Stefanucci and R. van Leeuwen, Nonequilibrium Many-Body Theory of Quantum Systems: A Modern Introduction, Cambridge University Press, ISBN 978-0-521-76617-3 (2013).
- [100] E. Gull, D. R. Reichman and A. J. Millis, Bold-line diagrammatic Monte Carlo method: General formulation and application to expansion around the noncrossing approximation, Phys. Rev. B **82**(7), 075109 (2010), doi:[10.1103/PhysRevB.82.075109](https://doi.org/10.1103/PhysRevB.82.075109).
- [101] D. A. Lidar, Z. Bihary and K. B. Whaley, From completely positive maps to the quantum Markovian semigroup master equation, Chemical Physics **268**(1), 35 (2001), doi:[10.1016/S0301-0104\(01\)00330-5](https://doi.org/10.1016/S0301-0104(01)00330-5).
- [102] C. Majenz, T. Albash, H.-P. Breuer and D. A. Lidar, Coarse graining can beat the rotating-wave approximation in quantum Markovian master equations, PHYSICAL REVIEW A p. 16 (2013).

- [103] R. S. Whitney, Staying positive: Going beyond Lindblad with perturbative master equations, J. Phys. A: Math. Theor. **41**(17), 175304 (2008), doi:[10.1088/1751-8113/41/17/175304](https://doi.org/10.1088/1751-8113/41/17/175304).
- [104] H. Aoki, N. Tsuji, M. Eckstein, M. Kollar, T. Oka and P. Werner, Nonequilibrium dynamical mean-field theory and its applications, Reviews of Modern Physics **86**(2), 779 (2014), doi:[10.1103/RevModPhys.86.779](https://doi.org/10.1103/RevModPhys.86.779).
- [105] O. Scarlatella, A. A. Clerk, R. Fazio and M. Schiró, Dynamical Mean-Field Theory for Markovian Open Quantum Many-Body Systems, Phys. Rev. X **11**(3), 031018 (2021), doi:[10.1103/PhysRevX.11.031018](https://doi.org/10.1103/PhysRevX.11.031018).
- [106] S. Flannigan, F. Damanet and A. J. Daley, Many-body quantum state diffusion for non-Markovian dynamics in strongly interacting systems, ArXiv210806224 Quant-Ph (2021).
- [107] M. Blume, V. J. Emery and A. Luther, Spin-Boson Systems: One-Dimensional Equivalents and the Kondo Problem, Phys. Rev. Lett. **25**(7), 450 (1970), doi:[10.1103/PhysRevLett.25.450](https://doi.org/10.1103/PhysRevLett.25.450).
- [108] A. J. Bray and M. A. Moore, Influence of Dissipation on Quantum Coherence, Phys. Rev. Lett. **49**(21), 1545 (1982), doi:[10.1103/PhysRevLett.49.1545](https://doi.org/10.1103/PhysRevLett.49.1545).
- [109] S. Chakravarty, Quantum Fluctuations in the Tunneling between Superconductors, Phys. Rev. Lett. **49**(9), 681 (1982), doi:[10.1103/PhysRevLett.49.681](https://doi.org/10.1103/PhysRevLett.49.681).
- [110] S. Chakravarty and A. J. Leggett, Dynamics of the Two-State System with Ohmic Dissipation, Phys. Rev. Lett. **52**(1), 5 (1984), doi:[10.1103/PhysRevLett.52.5](https://doi.org/10.1103/PhysRevLett.52.5).
- [111] A. J. Leggett, S. Chakravarty, A. T. Dorsey, M. P. A. Fisher, A. Garg and W. Zwerger, Dynamics of the dissipative two-state system, Rev. Mod. Phys. **59**(1), 1 (1987), doi:[10.1103/RevModPhys.59.1](https://doi.org/10.1103/RevModPhys.59.1).
- [112] M. Keil and H. Schoeller, Real-time renormalization-group analysis of the dynamics of the spin-boson model, Phys. Rev. B **63**(18), 180302 (2001), doi:[10.1103/PhysRevB.63.180302](https://doi.org/10.1103/PhysRevB.63.180302).
- [113] F. B. Anders and A. Schiller, Spin precession and real-time dynamics in the Kondo model: Time-dependent numerical renormalization-group study, Phys. Rev. B **74**(24), 245113 (2006), doi:[10.1103/PhysRevB.74.245113](https://doi.org/10.1103/PhysRevB.74.245113).
- [114] F. B. Anders, R. Bulla and M. Vojta, Equilibrium and Nonequilibrium Dynamics of the Sub-Ohmic Spin-Boson Model, Phys. Rev. Lett. **98**(21), 210402 (2007), doi:[10.1103/PhysRevLett.98.210402](https://doi.org/10.1103/PhysRevLett.98.210402).
- [115] R. Bulla, H.-J. Lee, N.-H. Tong and M. Vojta, Numerical renormalization group for quantum impurities in a bosonic bath, Phys. Rev. B **71**(4), 045122 (2005), doi:[10.1103/PhysRevB.71.045122](https://doi.org/10.1103/PhysRevB.71.045122).
- [116] M. Vojta, Numerical renormalization group for the sub-Ohmic spin-boson model: A conspiracy of errors, Phys. Rev. B **85**(11), 115113 (2012), doi:[10.1103/PhysRevB.85.115113](https://doi.org/10.1103/PhysRevB.85.115113).

- [117] L. Amico, H. Frahm, A. Osterloh and G. Ribeiro, Integrable spin-boson models descending from rational six-vertex models, Nuclear Physics B **787**(3), 283 (2007), doi:[10.1016/j.nuclphysb.2007.07.022](https://doi.org/10.1016/j.nuclphysb.2007.07.022).
- [118] A. Kopp and K. L. Hur, Universal and Measurable Entanglement Entropy in the Spin-Boson Model, Phys. Rev. Lett. **98**(22), 220401 (2007), doi:[10.1103/PhysRevLett.98.220401](https://doi.org/10.1103/PhysRevLett.98.220401).
- [119] Y.-H. Lee, J. Links and Y.-Z. Zhang, Exact solutions for a family of spin-boson systems, Nonlinearity **24**(7), 1975 (2011), doi:[10.1088/0951-7715/24/7/004](https://doi.org/10.1088/0951-7715/24/7/004).
- [120] A. W. Chin, J. Prior, S. F. Huelga and M. B. Plenio, Generalized Polaron Ansatz for the Ground State of the Sub-Ohmic Spin-Boson Model: An Analytic Theory of the Localization Transition, Phys. Rev. Lett. **107**(16), 160601 (2011), doi:[10.1103/PhysRevLett.107.160601](https://doi.org/10.1103/PhysRevLett.107.160601).
- [121] S. Bera, A. Nazir, A. W. Chin, H. U. Baranger and S. Florens, Generalized multipolaron expansion for the spin-boson model: Environmental entanglement and the biased two-state system, Phys. Rev. B **90**(7), 075110 (2014), doi:[10.1103/PhysRevB.90.075110](https://doi.org/10.1103/PhysRevB.90.075110).
- [122] D. P. DiVincenzo and D. Loss, Rigorous Born approximation and beyond for the spin-boson model, Phys. Rev. B **71**(3), 035318 (2005), doi:[10.1103/PhysRevB.71.035318](https://doi.org/10.1103/PhysRevB.71.035318).
- [123] Z. Lü and H. Zheng, Quantum dynamics of the dissipative two-state system coupled with a sub-Ohmic bath, Phys. Rev. B **75**(5), 054302 (2007), doi:[10.1103/PhysRevB.75.054302](https://doi.org/10.1103/PhysRevB.75.054302).
- [124] S. Florens, A. Freyn, D. Venturelli and R. Narayanan, Dissipative spin dynamics near a quantum critical point: Numerical renormalization group and Majorana diagrammatics, Phys. Rev. B **84**(15), 155110 (2011), doi:[10.1103/PhysRevB.84.155110](https://doi.org/10.1103/PhysRevB.84.155110).
- [125] A. Piñeiro Orioli, A. Safavi-Naini, M. L. Wall and A. M. Rey, Nonequilibrium dynamics of spin-boson models from phase-space methods, Phys. Rev. A **96**(3), 033607 (2017), doi:[10.1103/PhysRevA.96.033607](https://doi.org/10.1103/PhysRevA.96.033607).
- [126] K. Yang and N.-H. Tong, Equilibrium dynamics of the sub-ohmic spin-boson model at finite temperature*, Chinese Phys. B **30**(4), 040501 (2021), doi:[10.1088/1674-1056/abd393](https://doi.org/10.1088/1674-1056/abd393).
- [127] S. Wenderoth, H.-P. Breuer and M. Thoss, Non-Markovian effects in the spin-boson model at zero temperature, arXiv:2101.09463 [quant-ph] (2021).
- [128] A. Rivas, S. F. Huelga and M. B. Plenio, Entanglement and non-markovianity of quantum evolutions, Phys. Rev. Lett. **105**, 050403 (2010), doi:[10.1103/PhysRevLett.105.050403](https://doi.org/10.1103/PhysRevLett.105.050403).
- [129] G. Clos and H.-P. Breuer, Quantification of memory effects in the spin-boson model, Phys. Rev. A **86**(1), 012115 (2012), doi:[10.1103/PhysRevA.86.012115](https://doi.org/10.1103/PhysRevA.86.012115).
- [130] Á. Rivas, S. F. Huelga and M. B. Plenio, Quantum non-markovianity: characterization, quantification and detection, Reports on Progress in Physics **77**(9), 094001 (2014), doi:[10.1088/0034-4885/77/9/094001](https://doi.org/10.1088/0034-4885/77/9/094001).
- [131] C. H. Fleming and N. I. Cummings, Accuracy of perturbative master equations, Physical Review E **83**(3), 031117 (2011), doi:[10.1103/PhysRevE.83.031117](https://doi.org/10.1103/PhysRevE.83.031117).

- [132] D. Tupkary, A. Dhar, M. Kulkarni and A. Purkayastha, Fundamental limitations in Lindblad descriptions of systems weakly coupled to baths, Physical Review A **105**(3), 032208 (2022), doi:[10.1103/PhysRevA.105.032208](https://doi.org/10.1103/PhysRevA.105.032208).
- [133] A. González-Tudela and J. I. Cirac, Quantum Emitters in Two-Dimensional Structured Reservoirs in the Nonperturbative Regime, Phys. Rev. Lett. **119**(14), 143602 (2017), doi:[10.1103/PhysRevLett.119.143602](https://doi.org/10.1103/PhysRevLett.119.143602).
- [134] A. González-Tudela and J. I. Cirac, Markovian and non-Markovian dynamics of quantum emitters coupled to two-dimensional structured reservoirs, Phys. Rev. A **96**(4), 043811 (2017), doi:[10.1103/PhysRevA.96.043811](https://doi.org/10.1103/PhysRevA.96.043811).
- [135] A. González-Tudela and J. I. Cirac, Non-Markovian Quantum Optics with Three-Dimensional State-Dependent Optical Lattices, Quantum **2**, 97 (2018), doi:[10.22331/q-2018-10-01-97](https://doi.org/10.22331/q-2018-10-01-97).